2014

# LOW COST FLOW SENSING FOR FIELD SPRAYERS

Yue Zhang
*University of Kentucky*, yzh286@g.uky.edu

STUDENT AGREEMENT:

I represent that my thesis or dissertation and abstract are my original work. Proper attribution has been given to all outside sources. I understand that I am solely responsible for obtaining any needed copyright permissions. I have obtained needed written permission statement(s) from the owner(s) of each third-party copyrighted matter to be included in my work, allowing electronic distribution (if such use is not permitted by the fair use doctrine) which will be submitted to UKnowledge as Additional File.

I hereby grant to The University of Kentucky and its agents the irrevocable, non-exclusive, and royalty-free license to archive and make accessible my work in whole or in part in all forms of media, now or hereafter known. I agree that the document mentioned above may be made available immediately for worldwide access unless an embargo applies.

I retain all other ownership rights to the copyright of my work. I also retain the right to use in future works (such as articles or books) all or part of my work. I understand that I am free to register the copyright to my work.

REVIEW, APPROVAL AND ACCEPTANCE

The document mentioned above has been reviewed and accepted by the student's advisor, on behalf of the advisory committee, and by the Director of Graduate Studies (DGS), on behalf of the program; we verify that this is the final, approved version of the student's thesis including all changes required by the advisory committee. The undersigned agree to abide by the statements above.

Yue Zhang, Student

Dr. Timothy Stombaugh, Major Professor

Dr. Donald Colliver, Director of Graduate Studies

# LOW COST FLOW SENSING FOR FIELD SPRAYERS

---

THESIS

---

A thesis submitted in partial fulfillment of the requirements for the degree of Master of Science in Biosystems and Agricultural Engineering in the College of Engineering at the University of Kentucky

By
Yue Zhang
Lexington, Kentucky

Director: Dr. Timothy Stombaugh, Professor of Biosystems and Agricultural Engineering
Lexington, Kentucky

2014

**ABSTRACT OF THESIS**

LOW COST FLOW SENSING FOR FIELD SPRAYERS

Precisely measuring the flow rate in sprayers is a key technology to precision agriculture. With the development of advanced technologies, the demand for the ability to measure flow rate of individual nozzle has become more important and urgent.

This paper investigates the possibility of developing a low-cost flow rate measurement technique. The technique is based on analyzing the acoustic signal from a microphone placed near the nozzle tip. A comparison between acoustic signal and vibration signal was made to study the relations between them. Then several possible locations of the microphone for measuring flow rate were tested and compared, and one has been chosen as the best location. After that, two methods of analyzing data were proposed, one that could better describe the original curve was chosen. With all of that work done, further experiments were conducted on a variety of nozzle tips. The results showed that an acoustic sensor could be used as an indicator of flow rate from a nozzle, but that unique calibrations for different nozzle tips would be necessary.

KEYWORDS: Low-cost, Flow rate, FFT, Acoustics, Sprayer

Yue Zhang

January 6, 2015

# LOW COST FLOW SENSING FOR FIELD SPRAYERS

By

Yue Zhang

Yue Zhang, Student

Dr. Stombaugh, Major Professor

Dr. Donald Colliver, Director of Graduate Studies

01/07/2015

# ACKNOWLEDGEMENTS

I would like to extend my thanks to those who helped me not only in my master's project and thesis writing but also in my new life in the BAE department.

First I want to express my deep thanks to my advisor, Dr. Stombaugh, who gave me consistent help from the beginning of the project. I couldn't finish thesis without his instructions on the procedures and directions of the experiments, methods of result analysis and revisions of my thesis.

Next I want to thank Dr. Yongbo Wan for his generous help with my instrumentation work when I was confused about how to set up the equipment or how to continue my experiment.

Also I want to thank my committee members, Dr. Dvorak and Dr. Wu, for their reviews of my thesis and suggestions and questions which make me keep exploring in the research.

Finally, I want to thank my wife Huihui Yang for her encourage and support through my life and study.

# Table of Contents

# List of Tables

# List of Figures

# Chapter One: Introduction

## 1.1 Background Introduction

Conventional spraying technology is widely understood by farmers and manufacturers, yet the spray application process is attracting more and more attention from the agrochemical industry due to application efficiency and environmental impacts. The ability to precisely control and record the flow rate from the application machine is important.

A typical field sprayer will have a tank that will hold the diluted chemical to be applied. A pump will move the liquid from the tank through various plumbing, control valves, and manifolds to a series of nozzles distributed across a wide boom. Traditionally, it is impratical to actively control the flow rate at each nozzle in the spraying machines. Usually there is only one control valve and flow meter installed in the main feed line. Operators can only monitor and adjust overall flow rate. The system relies solely on uniformity between nozzle tips for even flow distribution.

Potential problems arise if a nozzle has been used for a long time and becomes worn. There may be some leakage, or corrosion of the orifice, or dirt particles may block the orifice, which will cause either more or less flow than expected. Besides, in some circumstances, the operator may want to vary the flow rate to different nozzles. For example, Fig 1.1 shows the situation when the spraying machines makes turns. The inner nozzle speed is smaller than the outer,

so the area covered by the inside nozzle will receive a higher application rate of chemicals than the outer area. To remedy this, the nozzles will be expected to have different flow rates.

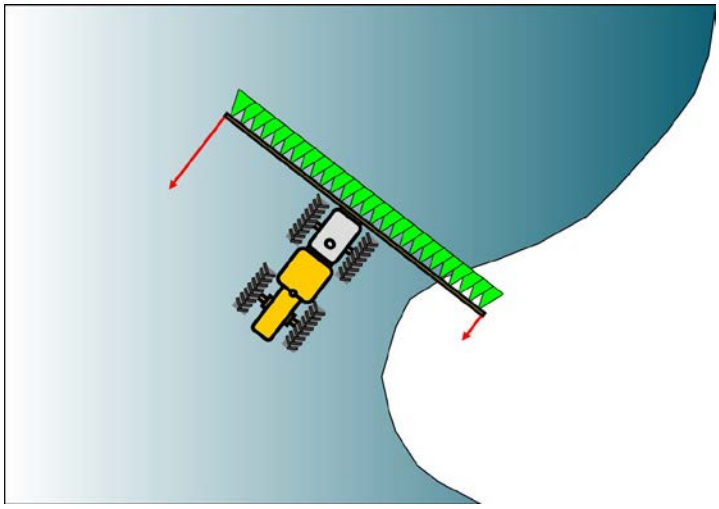

**Figure 1.1 Sketch of the spraying machine making turns**

One solution to this problem would be to install a flow rate sensor at each nozzle to facilitate nozzle-level control. Unfortunately current commercial sprayer models may have booms up to 36 m (approximately 120 ft) wide or wider. Typical nozzle spacing on the boom is 51 cm (20 in.), which means there would be 72 nozzles on a 36-m boom. To implement this level of control, it is important to reduce the cost of each sensor in order to control the machine. According to current technology, it is challenging to find a commercially available sensor at a reasonable price for the relatively low flow rates.

This paper introduces a new technique of measuring the flow rate through a single nozzle that balances the accuracy of the technology with the total cost of the device.

## 1.2 Literature Review

### 1.2.1 Control Technique Review

On a sprayer, the nozzle is the engineered orifice that creates a specific spray pattern as the liquid exists the sprayers. This research project utilized nozzles manufactured by Wilger (Lexington,TN). Figure 1.2 shows different typical nozzle configurations.

**Figure 1.2 Different Structures of Nozzle Tips**

Basically there are 3 levels of control that could be implemented on field sprayers. At the most basic level, the sprayer output is controlled by adjusting the system pressure. In this scenario, the forward velocity of the machine must be precisely controlled to maintain proper application rate. The second level of

control adds the function of automatically compensating for the machine velocity. The last one, which was the type that would be applied with this sensor, utilizes GPS control.

With the development of GPS technology, more and more machines now are using Automatic Section Control (ASC) technology. A GNSS-based guidance system is used to automatically turn sections of the machine on and off to keep the implement from overlapping adjacent swaths or other previously treated areas (Alabama A&M and Auburn Universities *et al.*, 2011). Advanced flow control is needed to achieve the control goal or rate. (Alabama A&M and Auburn Universities *et al.*,).

### 1.2.2 Flow Sensing Technique Review

There are many ways to measure the flow rate. The basic techniques can be categorized by the method of action, such as mechanical, pressure, optical, vortex and ultrasonic. (*Nick, 2012*)

It is suitable to measure the pressure drop to determine flow rate. Venturi tube and pilot tube devices use the pressure theory. A venturi tube has a smaller diameter part in the pipeline (Fig. 1.3). The smaller diameter section should between 0.224D and 0.742D. When the flow goes through the pipe, there would be pressure drop from the upstream to the downstream and the flow rate is proportional to the pressure difference.( *Asyiddin, 2007*)

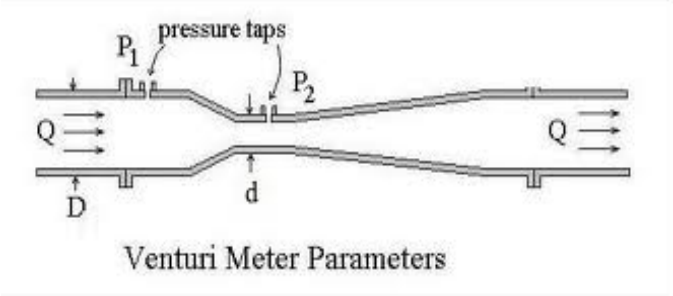


**Figure 1.3** The principle of the venture pipe (*Asyiddin, 2007*)

The venture pipe is widely used for clean, dirty or viscous fluid (*Sanjay Kumar, 2008*), but it is not suitable for this project since its size is always big compared with the one that is desired.

The Turbine flow meter uses the mechanical energy of the fluid to cause a vaned rotor to rotate (Fig. 1.4). It is an indirect sensor. The number of revolutions of the vane is proportional to the flow rate (*Frenzel, et al.,2011*). Signal receiving modules of the turbine flow meter sensors are installed outside of the flowing stream thus it doesn't have too many flow restrictions. The turbine flow meter is very expensive, so it might not be a good technique for out project.

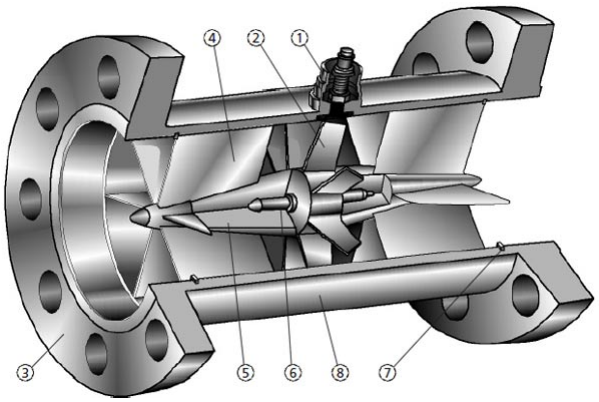


Figure 1.4 Inner structure of a turbine flow meter

Ultrasonic flow sensors (Fig. 1.5) capitalize on the impact of a moving fluid on an ultrasonic pulse sent though the flow stream (*Kumar, 2008*).

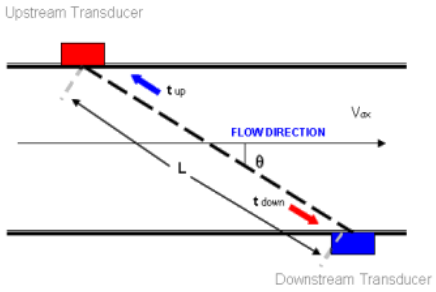


Figure 1.5 Sketch for the ultrasonic flow meter (Kumar, 2008).

The main method of detection is to measure the phase shift between the wave towards downstream and upstream (*John, 2013*). The equation for the measurement is:

$$v = \frac{KP^2}{2L}\left(\frac{1}{t_d - t_u}\right) \tag{1.1}$$

where K is a factor, P is the diagonal length between sensors, L is the horizontal distance between sensors, and $t_d$, $t_u$ represent transit time up and down stream (*N.Asyiddin, 2007*). Since the ultrasonic technique is used to detect signals with high more precision that far exceeds the cost requirement in this project, this sensor is not a good application here.

The vortex technique has grown into a major technique in the last 30 years (*Mattar and Vignos, Vortex Shedding Tutorial*). It uses a phenomenon called the

Karman effect, which means that when the flow passes by a bluff body it will create vortices downstream (Fig. 1.6); (*Yoder, 2010*).

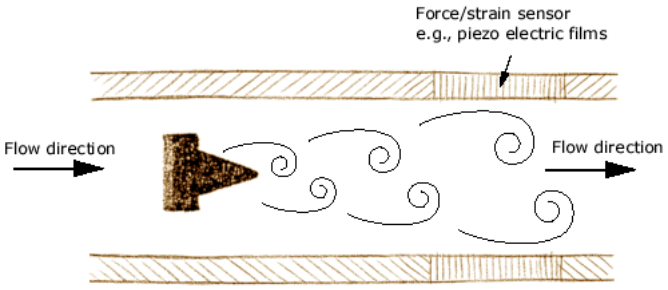


Figure 1.6 Karman effect and the principle of vortex flow meter (Yoder, 2010).

The frequency of the vortex is related to the flow rate, and the final equation for the flow meter is:

$$f = \frac{S_t.v}{d} \tag{1.2}$$

where the f is the frequency of the vortex, $S_t$ is the Strouhal number which is affected by materials, v is the fluid velocity and d is the pipe diameter (*Mattar and Vignos, Vortex Shedding Tutoria*). The vortex flow meter is widely used to measure flow but it will have problems for the low flow rates in this application since it would generate irregular vortices (*Yoder,2010*).

### 1.2.3 Research Work Review

There is still a lot of research being conducted by different research groups to improve the methods and make it more plausible to use vibration and acoustic signals to measure flow rate. One trial was conducted by *Balaje Dhanram*

*Ravichandran* (2002). The goal of that target was to monitor people's breath by investigating the sound from a whistle in their breath stream. They found a relationship between flow rate and frequency. Their method was verified by using pressure controlled air cylinders in a water bath maintained at 37 C, which is the same condition as human breath. The simulated breath went through the whistle where the outlet had been connected to a flow meter. The frequency response of the particular flow rate was recorded with a cell phone. An FFT algorithm was applied to analyze the data. The flow rate was adjusted by changing the pressure, and the frequency responses to different flow rates were recorded.

The principle was that when a person breathed through the pipe, it would cause resonance. The wavelength was fitted to the fundamental mode of the oscillation, which is $f = \frac{v}{4L}$, which resulted in the conclusion $f = \frac{v}{4(L + 0.4d)}$, where v is the acoustic velocity in the air, L is the length of the resonator, d is the diameter of the resonating material, and f is the Resonant Frequency that was tested.

Another use of acoustic signals to measure the flow rate was in nuclear technology (*Evans et al, 2002*). Without touching or interrupting the flow in a pipeline, they used an array of microphones on the pipe and an ultrasonic beam. The array of microphones was used to measure the reduction of wave numbers in the fluid in order to get the relationship between the flow rate and the change of the wave numbers. By a sequence of analysis, they concluded that：

$$\frac{\partial^2 y}{\partial t^2} = -Cp'(x), \tag{1.3}$$

where $C = \frac{g}{A\gamma}$, which meant that the flow acceleration was proportional to the pressure fluctuation. The next step was to look for the correlation of the standard deviation (std) of the pipe vibrations to the mean fluid flow rate. The velocity of fluids can be expressed as:

$$u = \bar{u} + u', \tag{1.4}$$

where $\bar{u}$ is the mean velocity and u' is the fluctuation velocity. What's more, they found that the oscillatory term $\bar{u}$ could be expressed as

$$\bar{u} = \sqrt{\bar{m}}, \tag{1.5}$$

where $\bar{m} = u'^2$. And they defined

$$\frac{\sqrt{\bar{m}}}{\bar{u}} = \sqrt{\frac{\bar{m}}{\bar{u}^2}}, \tag{1.6}$$

which was called *Intensity of Turbulence*.

Then by definition and calculation:

$$\frac{\sqrt{\bar{m}}}{\bar{u}} = \sqrt{\frac{\bar{m}}{\bar{u}^2}} = \frac{\frac{1}{N}\sum_{i=1}^{N}[u_i(t) - \bar{u}]^2}{\bar{u}^2} = C, \tag{1.7}$$

After some changes, they got:

$$\frac{1}{N-1}\sum_{i=1}^{N}[u_i(t)-\bar{u}]^2=\frac{NC}{N-1}\bar{u}, \tag{1.8}$$

where the left side was the definition of the sample standard deviation.

They used a PCB accelerometer to get the signal from the pipe. However, when they did a FFT transformation from time domain signals, they found that it had a very small shift of the peak frequency in the frequency domain. For example, at the flow rate of 1,311 lpm, the peak frequency occurred at 5.906 Hz, while at the flow rate of 4,161 lpm, the peak value occurred at 5.937 Hz, which was not a good reference. So they chose to analyze the signal noise, which was represented as the standard deviation of the frequency domain. At last, they found a nearly quadratic relation from the signal noise and the flow rate. The result would also be affected by pipe material and pipe diameter, but when one parameter was set, the result was always nearly quadratic.

*Kima et al. (2002)* proposed attaching an array of microphones to the pipe surface to measure the acoustic signal (Fig. 1.7). There was an acoustic source, a loud speaker, at one end and the other end was just a passive termination. They found the following relationship for how the sound propagated through the pipe:

$$P(f,x)=P^{+}(f)e^{(-j\gamma^{+}x)}+P^{-}(f)e^{(-j\gamma^{-}x)}, \tag{1.9}$$

where $P(f,x)$ is the frequency spectrum of the acoustic pressure at location x. $P^{+}(f)$ and $P^{-}(f)$ are the spectra of acoustic pressure downward and towards the

directions of the flow, respectively, and $\gamma^+$ and $\gamma^-$ were denoted as the propagation constants of the acoustic wave in each direction.

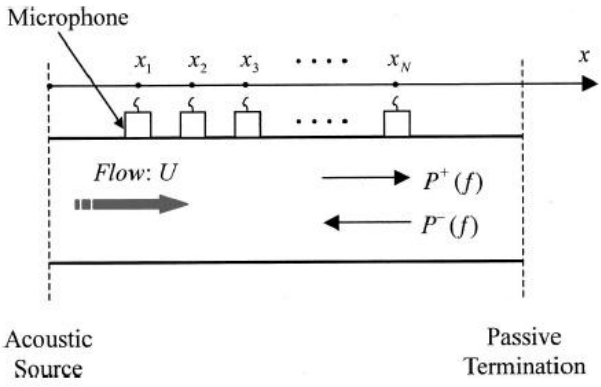


Figure 1.7 Experimental arrangement of microphone array on pipe as presented by Kima et al, 2002

Through calculation, they concluded that flow rate in the pipe can be measured with the variables of the wave number, k, and the difference between the wave numbers in the downstream and upstream directions. Finally, the Volume Flow rate, Q, is described as:

$$Q = \frac{-(k_0+\sigma)+\sqrt{(k_0+\sigma)^2+4(\angle G_1/2\Delta x)}}{\angle G_1/\Delta x}\frac{\pi d^2}{4}c_0, \qquad (1.10)$$

where $\Delta x$ was the distance between two consecutive sensors, k was for the wave number, $k_0$ was the free medium wave number, and $\sigma$ represented the attenuation constant.

In 2012, *Kakuta et al.* did some research to develop a vibration sensor with wide frequency range using a microphone (Fig.1.8). They stated that the

velocity of a point in the fluid was regarded as the superposition of an average value $\bar{u}$ and fluctuating value $u'$. The velocity was represented as $u = \bar{u} + u'$, where $\bar{u}$ and $u'$ were calculated with adequately long T as follows:

$$\bar{u} = \frac{1}{T}\int_0^T u.dt\,, \tag{1.11}$$

$$u' = \frac{1}{T}\int_0^T u'.dt\,, \tag{1.12}$$

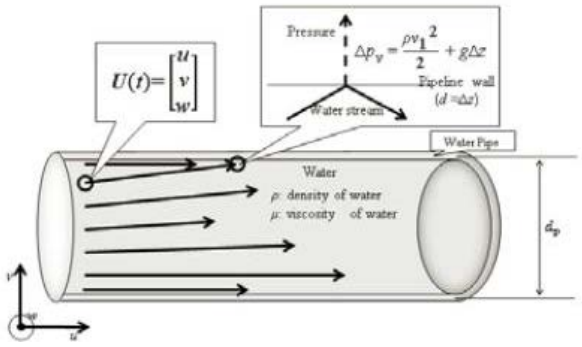


Figure 1.8 Water velocity model in the pipe (Kakuta et al,2012)

They also defined the flow in the horizontal direction w and gravity direction v:

$$\bar{w} = \frac{1}{T}\int_0^T w.dt\,, \tag{1.13}$$

$$w' = \frac{1}{T}\int_0^T w'.dt\,, \tag{1.14}$$

$$\bar{v} = \frac{1}{T}\int_0^T v.dt\,, \tag{1.15}$$

$$v' = \frac{1}{T}\int_0^T v'.dt\,, \tag{1.16}$$

So the velocity component, w, near the nozzle wall was 0 because it was stopped by the wall. In this model, the water flow velocity obeyed the Bernoulli's principle as expressed in:

$$\frac{v^2}{2} + \frac{p}{\rho} + gz = const \quad , \tag{1.17}$$

Suppose the internal pressure were $p_{v1}$ and $p_{w1}$, external pressure on the pipe wall were $p_{v2}$ and $p_{w2}$. $v_2$ and $w_2$ should be omitted because $v_2$ and $w_2$ are 0.

$$\frac{v_1^2}{2} + \frac{p_{v1}}{\rho} + gz_1 = \frac{p_{v2}}{\rho} + gz_2\,, \tag{1.18}$$

$$\frac{w_1^2}{2} + \frac{p_{w1}}{\rho} = \frac{p_{w2}}{\rho}\,, \tag{1.19}$$

Substituting $\Delta p_v = p_{v2} - p_{v1}, \Delta p_w = p_{w2} - p_{w1}$, $\Delta z = z_2 - z_1$, then they became:

$$\Delta p_v = \frac{\rho v_1^2}{2} + g\Delta z\,, \tag{1.20}$$

$$\Delta p_w = \frac{\rho w_1^2}{2}\,, \tag{1.21}$$

Then the flow velocity was shown as:

$$u_1 = 2\sqrt{2\frac{\Delta p_u}{\rho}}\ , \tag{1.22}$$

$$v_1 = 2\sqrt{2\frac{\Delta p_v - g\Delta z}{\rho}}\ , \tag{1.23}$$

$$w_1 = 2\sqrt{2\frac{\Delta p_v}{\rho}}\ , \tag{1.24}$$

Therefore the relationship between energy and velocities was:

$$U(t) = \sqrt{u^2 + w^2 + v^2} = \sqrt{\frac{2}{\rho}(\Delta p_v + \Delta p_u + \Delta p_w - g\Delta z)}\ , \tag{1.25}$$

Next they got the relation of flow rate Q with pressure fluctuation:

$$Q = C_l \frac{d_p{}^2}{2}\pi\sqrt{2\frac{\Delta p_u}{\rho}}\qquad , \tag{1.26}$$

Based on the equations above, they developed a sensor enclosed with a microphone. The structure of the sensor was described. They covered the chamber with pressurized film to enclose atmospheric pressure in the chamber so it could be used as a vibration sensor. The pressurized film was caused to vibrate by input vibration. The vibration would be transferred to an air spring through internal atmosphere pressure variations.

The above advanced experiments are still in experimental phases. Thus for this application, it was necessary to find another way to detect the flow rate.

# Chapter Two: Objectives

## 2.1 Introduction

The goal of this project was to design a low cost flow rate sensor that could be used at the nozzle level on an agricultural field sprayer. Current flow rate sensors are very expensive so only one sensor is typically used on the machine to monitor the flow rate of the whole system. Because there can be flow rate fluctuations between nozzles, it is desirable to monitor the flow at each nozzle. The sensor developed in this project would be inexpensive enough to replicate across the spray boom. The sensor should be robust with respect to disturbance rejection even with bad conditions typical for agricultural field machinery, and it should relatively high precision.

*Objective1. Comparing two methods: Vibration and Acoustics*

When liquid flows through the pipes and the nozzle on the sprayer, it will cause vibration of the pipe and acoustics vibration, which is the combination of the friction and vortices in the flow. The first objective was to determine whether these two vibration modes and resultant frequencies were the same. After comparing the vibration and acoustic signals, the best measurement method was selected according to the resolution, cost, size, etc.

*Objective2. Comparing different places for mounting the sensors*

After determining the best sensing method to apply to this project, repeated experiments were conducted to determine the best location for the sensor

relative to the nozzle. These tests were all conducted using one common nozzle tip.

*Objective3. Choosing the appropriate technique to process the data*

After choosing the best location for the sensor, more repeated experiments were conducted to determine a robust calibration of the sensor for flow rate measurement. Several different data processing techniques were introduced and applied to select the most appropriate relationship between sensor output and flow rate.

*Objective4. Apply the technique to several selected nozzles*

Once the characteristic relationship for a single nozzle tip was determined, the experiments were repeated with different commonly used nozzle tips. The same relationships were applied to see if the calibrations were valid only for a single nozzle or if they could be applied across a broader range of nozzle tips.

# Chapter Three: Tests with Acoustic Signal and Vibration Signal

## 3.1 Description

The first objective of this project was to consider whether the acoustic signal from the nozzle was the same as vibration of the surface of the nozzle body and tip. If they were the same, it could be easy to study the acoustic signal by studying the vibration signal measured with a familiar accelerometer. On the other hand, if the acoustic signal was different from vibration signal, then there would be a need to consider the essentials of these signals. What did they stand for? What was the difference between them? Which one of them would have a greater potential for indicating nozzle flow rate performance?

This part of the project focused on measuring flow rate using a microphone and an accelerometer. These two sensors were tested at the same location relative to the nozzle and the results were compared in the frequency domain. This sensor comparison was used to understand the meaning of the signals, and to figure out what caused the differences. Finally, a conclusion was reached as to whether these two methods would lead to the same results and which method was preferred for this project.

### 3.1.1 Methods and Materials

*Materials*

Figure 3.1 shows the test bench which was used in the experiments. It consisted at a section of a boom from a commercial sprayer. The boom section

had four nozzles on it, but only one was used in the experiment. A pump and supply tank were used to deliver water to the boom. A flow control valve (Model LCR05LPM, Alicat Scientific, Tucson, AZ) was used to control the flow of water to the nozzle.

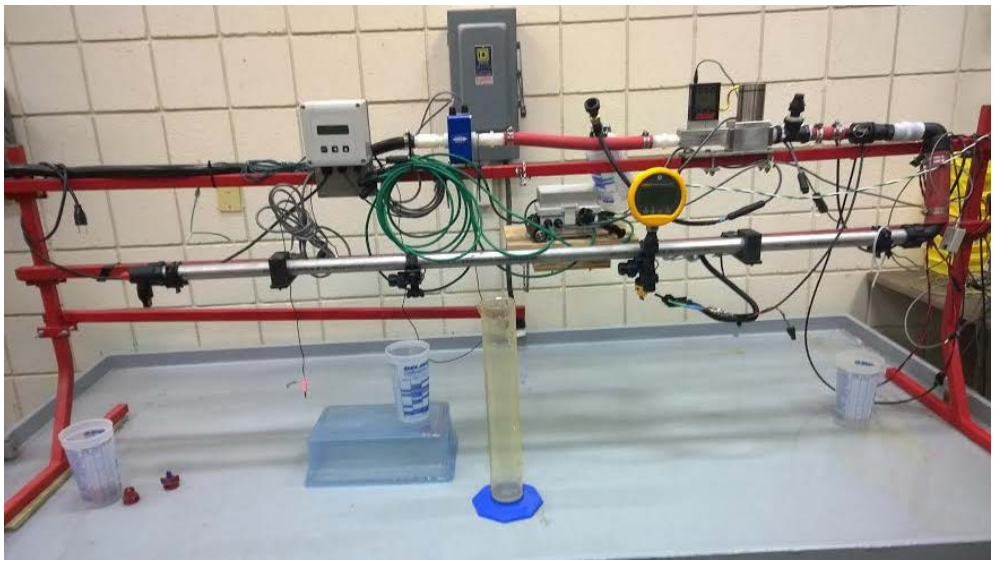

Figure 3.1 Overview of the Test Bench

The following sensors were used in this part of the study:

Microphone: BL-21994-000(Knowles, Itasca,IL)

Accelerometer: ADIS 16228 (Analog Devices, with ADISUSBZ kit)

DAQ Board: NI-USB 4431(National Instrument, Austin,Tx)

Nozzle: DR80-04(Wileger Industrial Ltd., Lexington,TN)

Software: LabVIEW, Matlab, ADIS 16228 Evaluation Software, NI-MAX

### 3.1.2 Data Acquisition Board Setup

In this project, a specialized data acquisition (DAQ) board was used to collect the data for analysis. The benefit of using a DAQ board is that the microphone acquisition could be clearly controlled for confidence in voltage vs. sound pressure level calibration and frequency sampling. Considering the compatibility with LabVIEW, the NI-USB 4431 from National Instrument was chosen (Fig. 3.2). It has 4 24-bit analog inputs and 1 24-bit analog output where all of them are BNC connections. The sampling rate could be as high as 102.4 kS/s. Also the input coupling mode has AC/DC selections.

Figure 3.2 NI-USB 4431 Data Acquisition Board

The NI-USB 4431 is good for sound and vibration acquisition because of following reasons:

1. It has high sampling rates (up to 102.4 kHz) which meant that the signal frequency could go up to 51.2 kHz without aliasing.
2. NI has provides Sound and Vibration assistant software, which could automatically do signal analyses such as filtering, windowing, averaging and time and frequency domain analysis.

The NI-USB 4431 was powered by USB bus, so once connected with PC, it was powered automatically. When the board is connected with PC, it will

automatically install the drives and related software. For this project, the AC coupling mode was chosen, and the sampling rate was set to the highest, which was 100 kHz.

### 3.1.3 Microphone Setup

In this test, a Knowles BL-microphone was used (Fig. 3.3). It is a high quality microphone that gave relatively precise and reliable results. The following specific tasks were completed to initialize and use the microphone.

1. A source following circuit (Fig. 3.4) was constructed based on suggestion from the manufacturer literature.
2. The output of the circuit was connected to the DAQ board and the USB output of the DAQ board was connected to PC.
3. A LabVIEW VI was created to interface with the DAQ and control data acquisition.

Figure 3.3 Knowles BL-21994

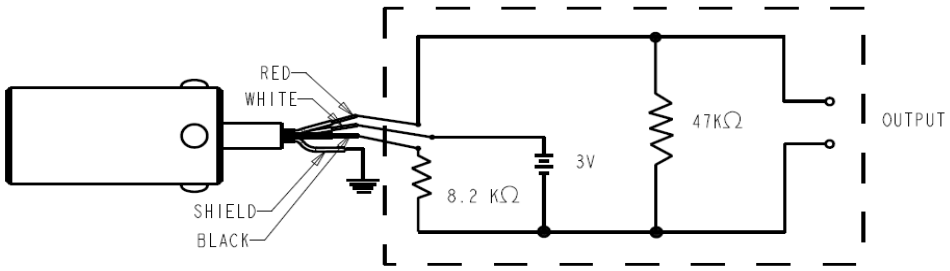


Figure 3.4 Source Following circuit for BL-21994

### 3.1.4 Accelerometer Setup

The ADIS 16228 (Fig. 3.5) was a complete vibration sensing system that combined triaxial acceleration sensing with advanced time domain and frequency domain signal processing. Frequency domain processing included a 512-point, real-valued FFT for each axis, along with FFT averaging, which reduced the noise floor variation for finer resolution (ADIS 16228 Datasheet). The sensor itself had an SPI port to communicate data and commands with an ADISUSBZ kit (Fig. 3.6), which converted the SPI signal to a USB signal that could be connected to the data acquisition PC. Evaluation software provided with the accelerometer was used to automatically generate the frequency plots and control the accelerometer.

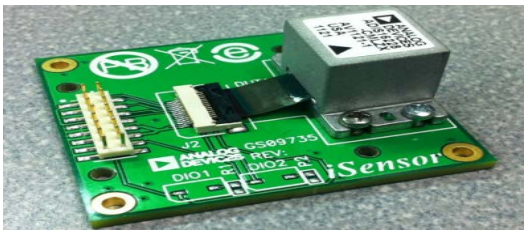


Figure 3.5 ADIS 16228 accelerometer with connecting board

Figure 3.6 ADIS 16228 SPI to USB communication kit

There were 4 modes of operation for the accelerometer for different purposes: Manual FFT mode, Automatic FFT mode, Manual Time capture mode, Real-Time mode. The mode was selected by setting the REC_CTRL1 register (Base Address=0x1A) to the correct value (Table 3.1). In this test, only the Manual FFT was used. Once a new flow rate was set, a command on the VI was used to trigger periodic acquisition of a spectral record.

Table 3.1 Configuration modes for the ADIS 16228 accelerometer.

| REC_CTRL1[1:0] | MODE |
|---|---|
| 00 | Manual FFT mode |
| 01 | Automatic FFT mode |
| 10 | Manual Time capture mode |
| 11 | Real-Time mode |

The accelerometer was mounted on one side of the nozzle body with electrical tape. The accelerometer had to be fastened directly to the surface of the nozzle body; otherwise, the vibration signal would attenuate dramatically. The single or tri-axis FFT data collected through the ADISUSBZ were saved to a spreadsheet file for further processing and analysis.

## 3.2 Experiments

### 3.2.1 Tests with accelerometer

The first task was to use the accelerometer to measure nozzle vibration. Three groups of tests were designed. In each group, five different tests were conducted for flow rates from 1.20 lpm to 1.60 lpm. The differences between the five groups were the sampling frequency and dynamic range. The settings are summarized in Table 3.2. Since the number of sampling points was the same (10240) it was easy to figure out the frequency range that might be helpful.

Decreasing the dynamic range increased the dynamic measurement accuracy. Because the nozzle vibration was expected to be very tiny, the smallest range (0-1 g) was chosen to insure the best resolution.

Table 3.2 The configuration of sampling rate and range for 3 tests

| Test Number | Sampling Frequency (Hz) | Dynamic Range (g) |
|---|---|---|
| Test 1 | 1280 | 0-1 |
| Test 2 | 5120 | 0-1 |
| Test 3 | 10240 | 0-1 |

The results of the experiments (Fig. 3.7-3.9) showed the sensitivity of the noise to the flow rate and the trend of the vibration amplitude to the flow rate. It was observed that the accelerometer was very sensitive to noise. From test 1, two peaks were observed between 0- 200 Hz. Beyond 400 Hz there was too much noise; thus, it was better to focus on the peaks below 200 Hz. As the sampling frequency was increased (Fig. 3.7, 3.8), the frequency response became very noisy.

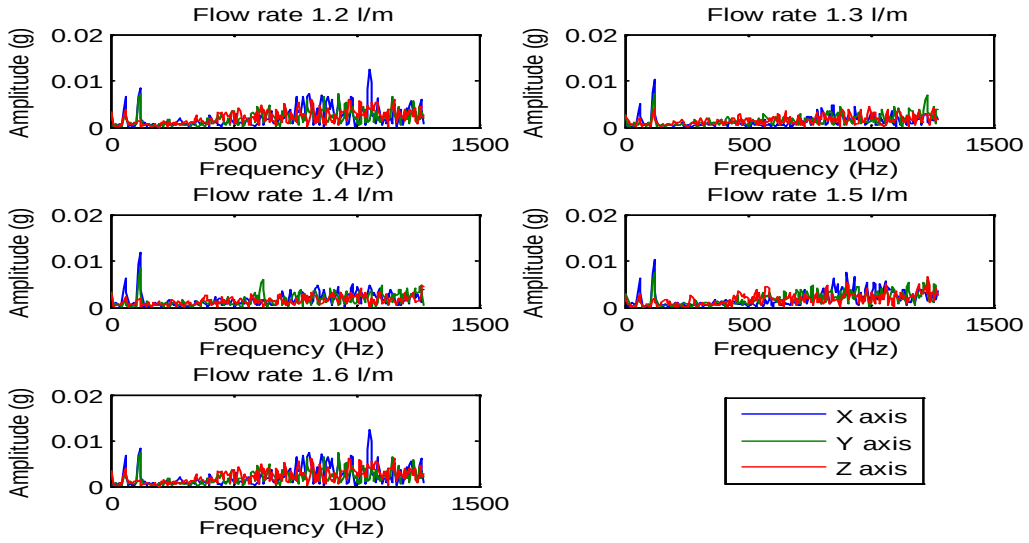


Figure 3.7 FFT of Accelerometer output with sampling rate of 1280 Hz

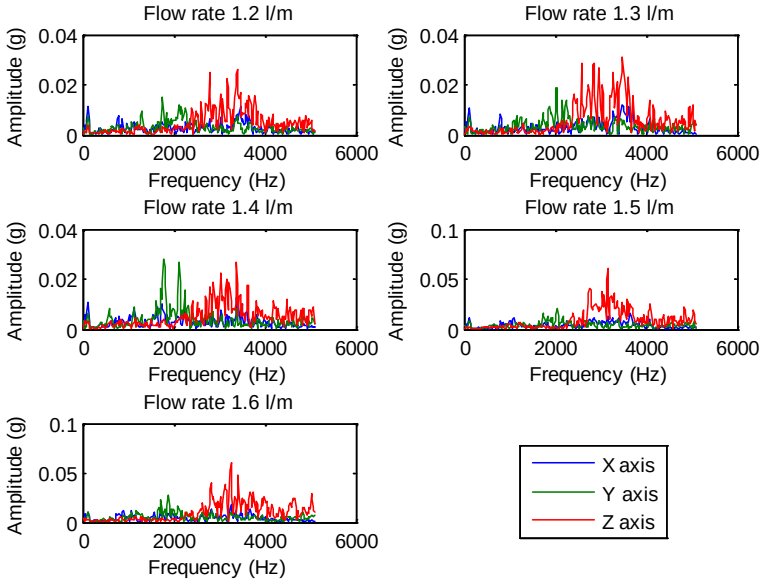


Figure 3.8 FFT of Accelerometer output with sampling rate of 5120 Hz

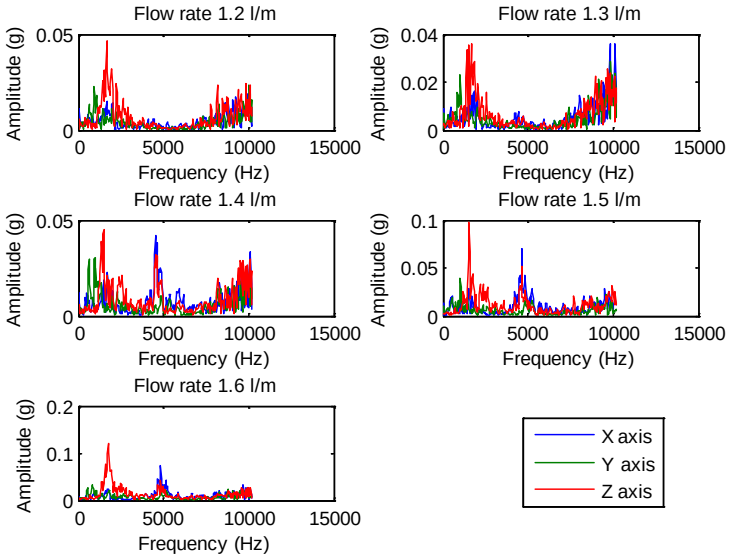


Figure 3.9 FFT of Accelerometer output with sampling rate of 10240Hz

When the sampling frequency was low, the dominant vibration was the X axis, but after the sampling rate increased, the dominant vibration became the Z axis. This meant that the vibration on Z axis was dominated by high frequency while in the low frequency range, the vibration on X axis was more notable. And in the low frequency, the peak frequency happened to be the same in 3 axes.

Then it was important to compare two peak frequencies below 200 Hz for the different flow rates (Table 3.3). Interestingly, the two peaks did not shift with the flow rate. The first peak was power inference, which will be discussed further in Chapter 5. Thus, no shift in peak frequency happened for the vibration of the nozzle when the flow rate increased.

Table 3.3 Two peak frequency of different flow rate before 200 Hz

| Flow Rate (lpm) | 1st Peak frequency (Hz) | 2nd Peak frequency (Hz) |
|---|---|---|
| 1.2 | 60 | 120 |
| 1.3 | 60 | 120 |
| 1.4 | 60 | 120 |
| 1.5 | 60 | 120 |
| 1.6 | 60 | 120 |

### 3.2.2 Tests with microphone

In order to compare with the vibrations measured by the accelerometer, the microphone was fastened at the same location on the surface of the nozzle body but held off of the surface by a very short distance. This distance was necessary because the sound pressure level at the sound source will go to infinity and that could damage the microphone. The flow rate was varied from 1.20 lpm to 1.60 lpm as the spectral signatures were recorded. The frequency range that was measured was from 0- 24000 Hz, which was far more than the limit of the microphone (10000 Hz).

Figure 3.10 shows the frequency response for 5 different flow rates. Comparing the audio signal with the vibration signal, the audio signal did not appear to have as much noise even at the high sampling frequency.

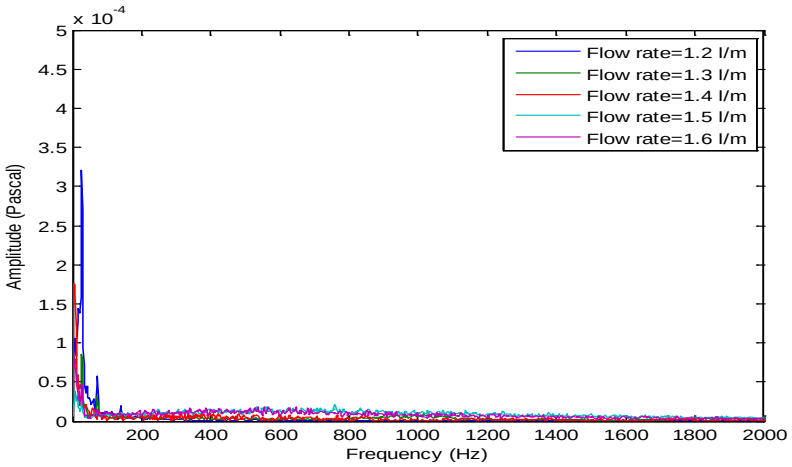


Figure 3.10 FFT of microphone output of flow rates from 1.2 lpm to 1.6 lpm

Next was to compare the result at the same flow rate. Since only the lower frequency range signals were affected by flow rate, plotting the response before 1000 Hz was sufficient (Figs. 3.11-3.15). The comparison showed that the vibration from the nozzle body and the acoustic vibration were not the same.

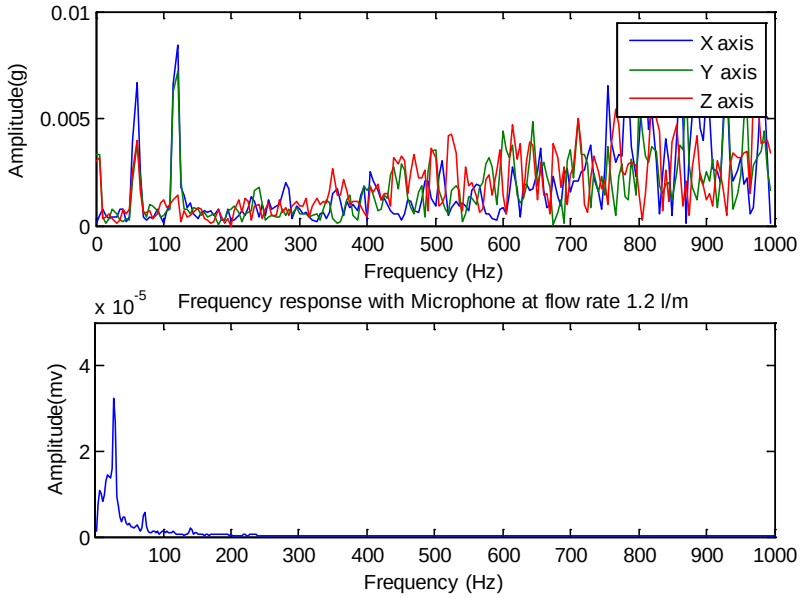


Figure 3.11 Comparison of accelerometer (top) and microphone (bottom) results at a flow rate of 1.2 lpm.

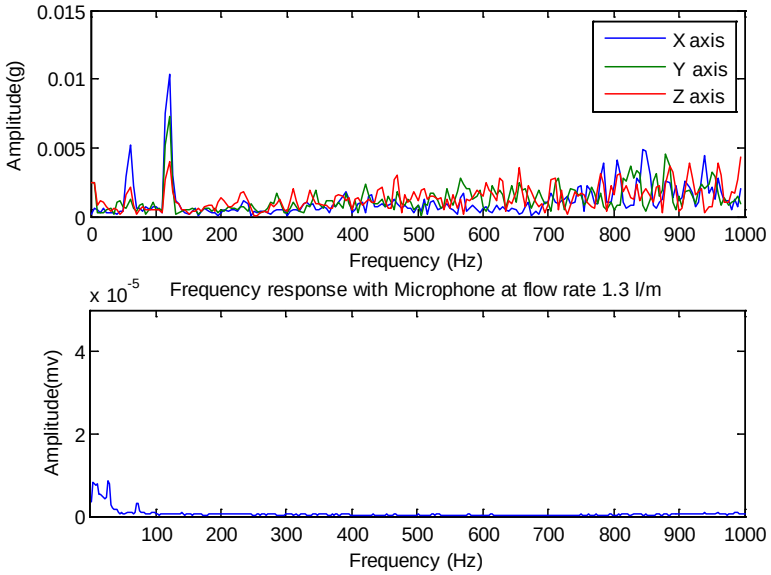


Figure 3.12 Comparison of accelerometer (top) and microphone (bottom) results at a flow rate of 1.3 lpm

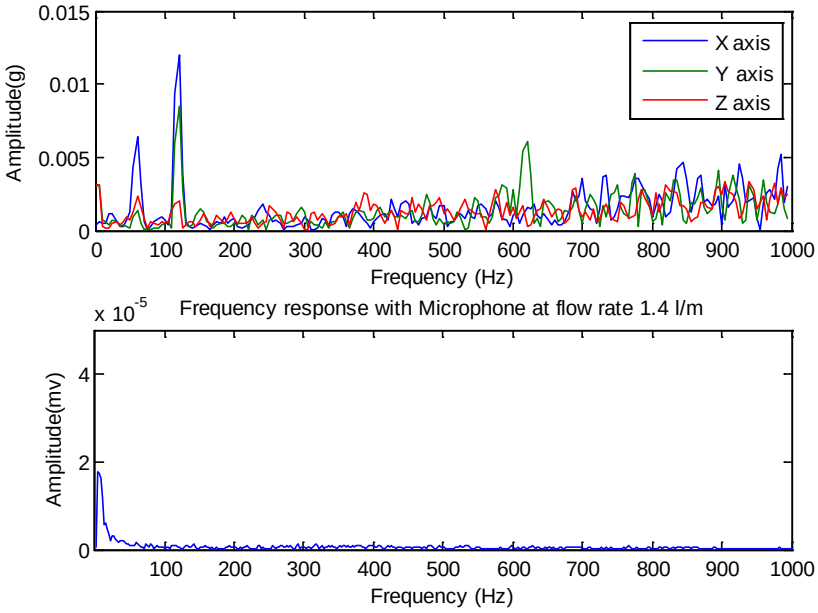


Figure 3.13 Comparison of accelerometer (top) and microphone (bottom) results at a flow rate of 1.4 lpm

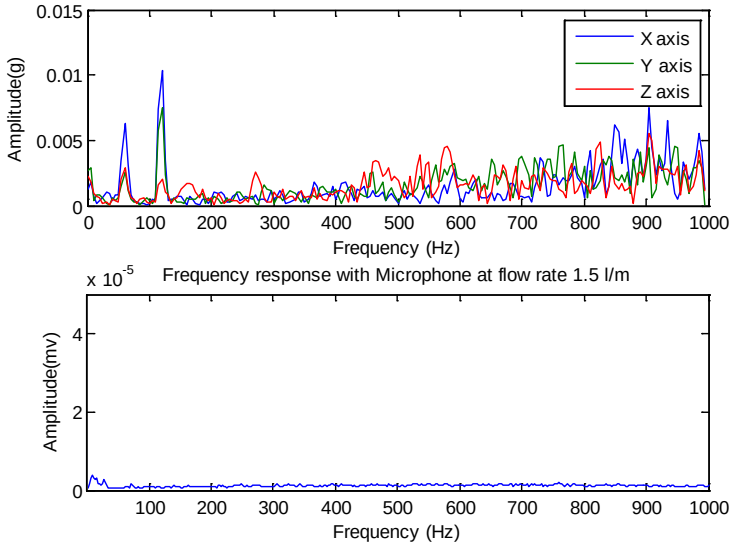


Figure 3.14 Comparison of accelerometer (top) and microphone (bottom) results at a flow rate of 1.5 lpm

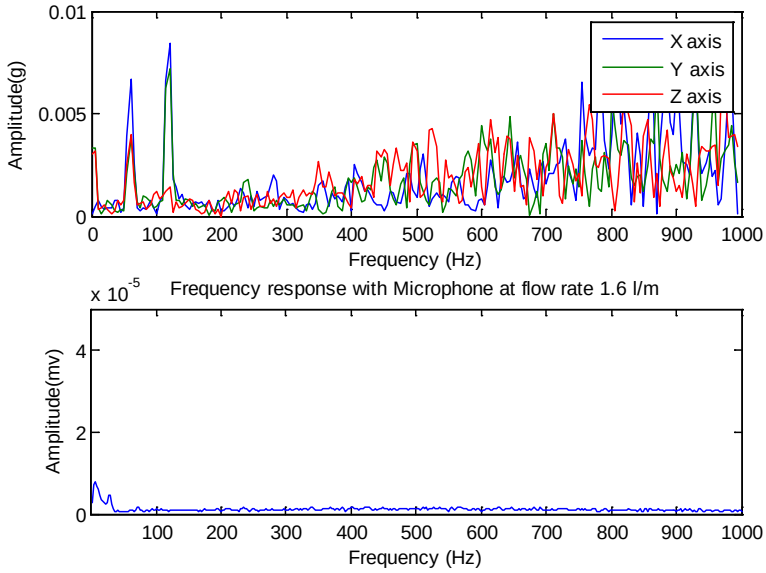


Figure 3.15 Comparison of accelerometer (top) and microphone (bottom) results at a flow rate of 1.6 lpm

## 3.3 Summary and Conclusions

In this chapter, the work focused on comparing two potential methods of characterizing flow rate through a nozzle: testing the nozzle vibration by accelerometer and testing the acoustic vibration by microphone. The first task was to see if the two vibrations are the same. By comparison, it was found that that the results were not the same, which meant that the two vibration modes were not the same.

Secondly, it was important to know the source of the vibration. By using the accelerometer, the flow through the nozzle caused vibration, and that vibration was transmitted to the accelerometer, so what it measured was the vibration of the nozzle itself. However, what the microphone received was the air vibration

caused by the nozzle vibration. Once the nozzle shakes, the air in the gap between the nozzle surface and microphone would vibrate, so the microphone would detect the air vibration. That would explain why the results were different.

Finally, the selection that would be put into use was the microphone because its output was changing with flow rate. Also the cheapest accelerometer would cost around 40 dollars while the microphone would only cost about 2-3 dollars each, so using microphone would be more reasonable in a multiple-nozzle application.

# Chapter Four: Choosing the Location of Microphone

## 4.1 Description

In last chapter, two methods of measuring nozzle flow rate were compared, and measuring the acoustic vibration was chosen as the best method to be applied in this project. The next question to be answered was where should the sensor be located? This chapter addresses choosing the best location for the sensor relative to the nozzle body and nozzle tips.

The distance between the nozzle and microphone had great influence on the result. If the microphone was too far away, the acoustic signal in the air would attenuate soon, so the signal the microphone received might be very tiny and not good for detecting and analyzing. If the sensor was attached close to the nozzle tip, it would be damaged by water or at least affected by water drops. It was also important to consider the cost of manufacturing a mounting system for the microphone, especially if the microphone was integrated with the nozzle body or tip.

The following factors needed to be taken into consideration: manufacturing cost, avoiding water damage, and maintaining ample signal intensity. This chapter describes a series of tests that were conducted to determine the best location for the microphone relative to the nozzle.

### 4.1.1 Materials and Methods

*Microphone:* BL-21994-000(Knowles, Itasca, IL)

*Software:* Matlab, Labview, Pro/e

*Nozzle Tip:* Wilger MR80-04

The setup of the equipment and software was described in Chapter 3.

*Method:*

To determine the best location for the microphone, the following specific tasks were completed.

a) Identify the possible positions for the microphone on or around the nozzle.
b) Record the acoustic signature for different flow rates at each of the chosen locations.
c) Analyze and compare the results to determine the best location for further testing.

## 4.2 Experiments

### 4.2.1 Selecting the possible positions

Three possible locations for the microphone relative to the nozzle tip were identified (Fig 4.1). Since the nozzle tip was symmetrical, it was assumed that the acoustic signal transmitted in opposite directions would be identical; thus, only one octant needed to be considered, which reduced the number of experiments necessary.

Within octant 1, several places were selected to test the sensor. Location A was a place just above the nozzle tip. Location B was just below the tip but close to the spray pattern surface. Location C was in the same horizontal plane with the nozzle tip.

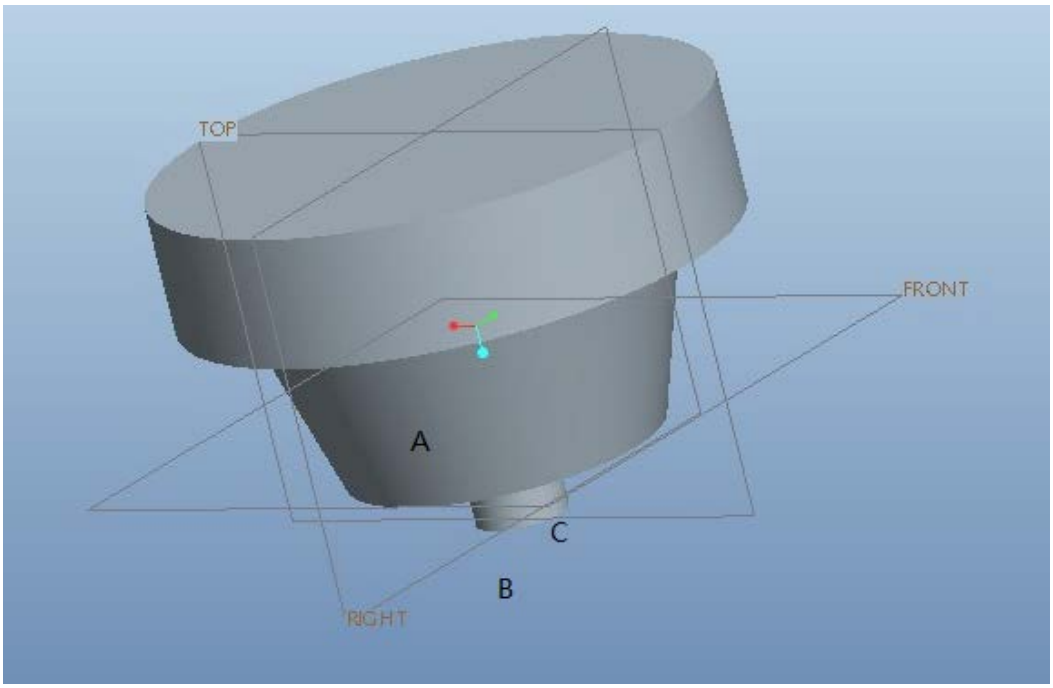


Figure 4.1 Sketch of typical nozzle tip showing three possible locations for microphone sensor.

### 4.2.2 Evaluation of position A

The sensor was tested at position A, which was extremely close to the surface of the nozzle body but not attached to it as described in Chapter 3. As suspected, the acoustic vibration was very tiny there because the shell of the nozzle was solid and the air vibrations caused by the nozzle were very small.

Five tests were conducted using the microphone at flow rates from 1.2 lpm to 1.6 lpm. The frequency response plot (Fig. 4.2) did not show any trend or correlation to the flow rate. The lowest flow rate had the highest amplitude of the peak frequency while at 1.4 lpm, the peak frequency amplitude was the lowest.

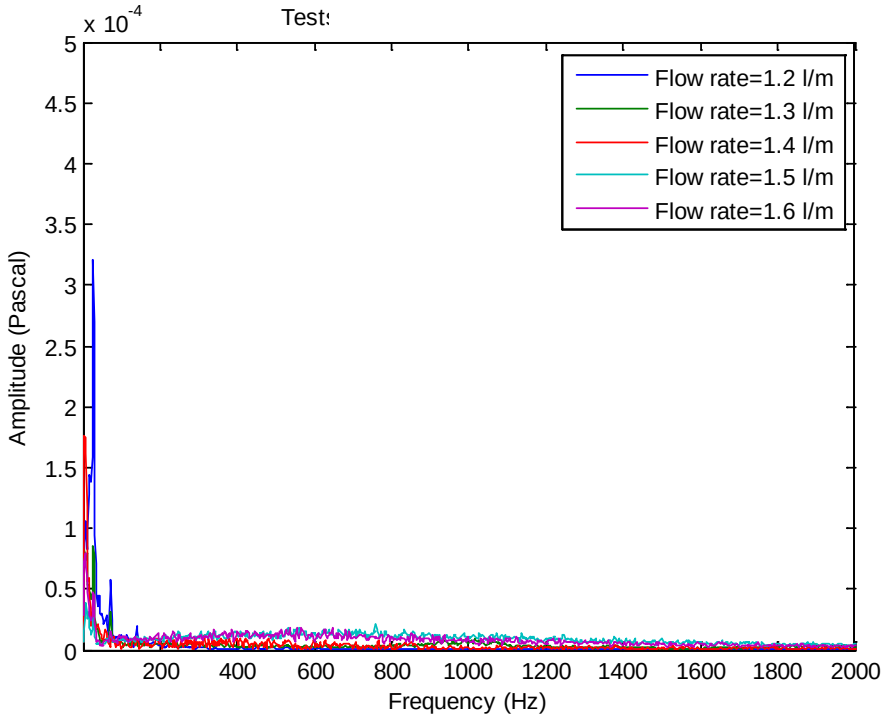


Figure 4.2. Audio frequency response with sensor located at position A.

The average sound pressure plot (Fig. 4.3) still showed that when the flow rate increased, the average pressure did not change with the same trend as flow rate. Thus, it is not good to put the sensor at location A since it gave too little information to indicate flow rate.

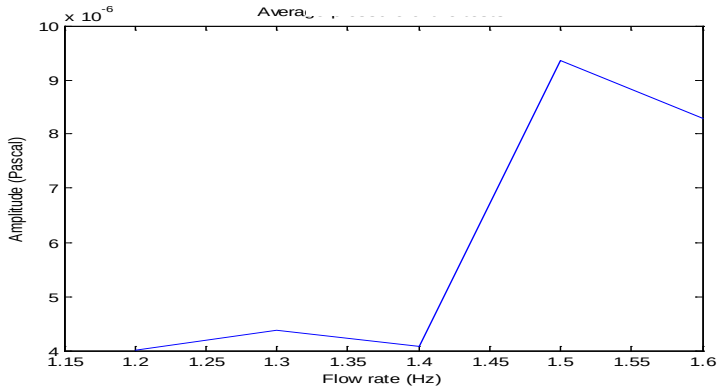


Figure 4.3 Average amplitude at different flow rates.

### 4.2.3 Evaluation of position B

Position B was a very important position to consider since it was easy to manufacture and convenient to measure the flow. Thirteen tests were conducted at flow rates from 1.0 lpm to 2.2 lpm. The frequency response (Fig. 4.4) showed a high response to flow rate at frequencies below 5000 Hz but quite low response afterwards. So a new plot of the frequency response was split before 5000 Hz (Fig. 4.5).

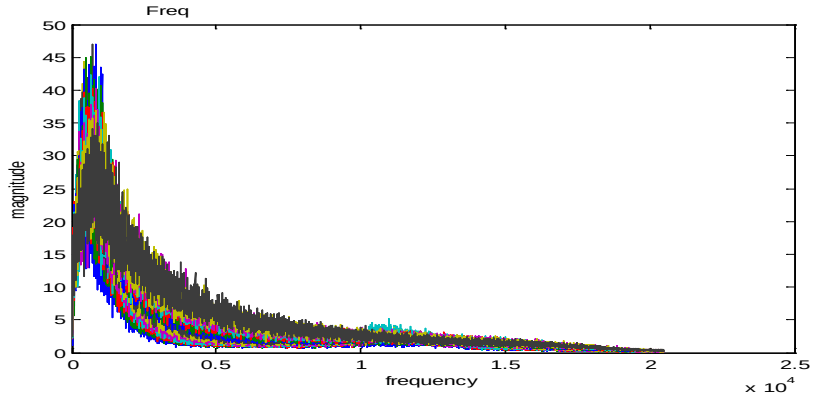


Figure 4.4 Frequency response at location B

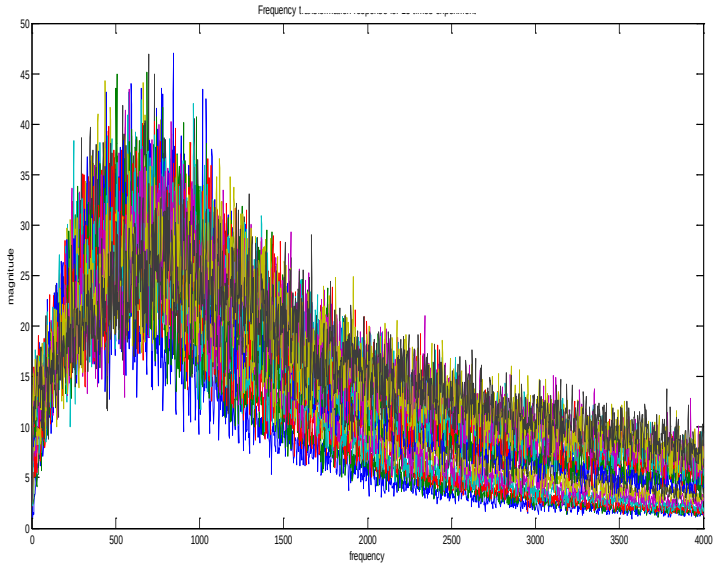


Figure 4.5 Frequency response at location B

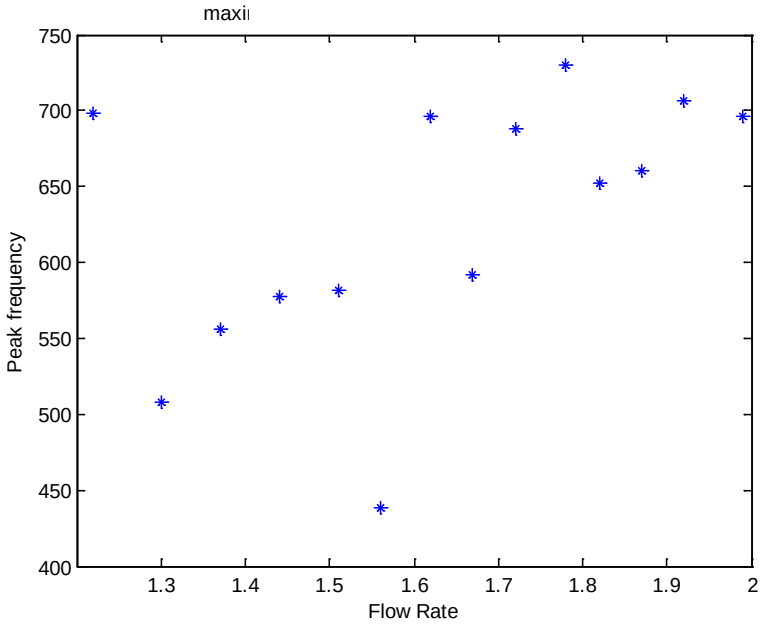


Figure 4.6 Maximum frequency in 400-800 Hz

The next task was to look at the power for the frequency signal. From the previous result it was known that most of the power was concentrated below 5000

Hz. It was important to calculate the power of the signal from 0–5000 Hz. In practice, it would be computationally expensive to calculate the power of the acoustic signal, so only the mean value and standard deviation of the signal were calculated. The standard deviation of the acoustic signal represented the variation from the mean value. Fig 4.6 shows that the peak frequency at each flow rate was concentrated in the range between 450 Hz and 750Hz, which was relatively low in the frequency domain.

The mean value of the signal first increased with flow rate and then decreased at the flow rates above 1.72 lpm (Fig. 4.7). This would not be a good indication of flow since it would not have a one-to-one mapping from flow rate to mean value. A concern was that the microphone might be getting wet from water spray. The experiments was redone and the microphone was dried when the flow rate reached 1.72 lpm. The results (Fig. 4.9) showed a better relation. After drying the microphone, the mean value showed an increasing trend. It was obvious that the water was damping the sensor making the results not consistent. Since it was necessary to keep the sensor dry all the time, position B was not a very good place for the sensor.

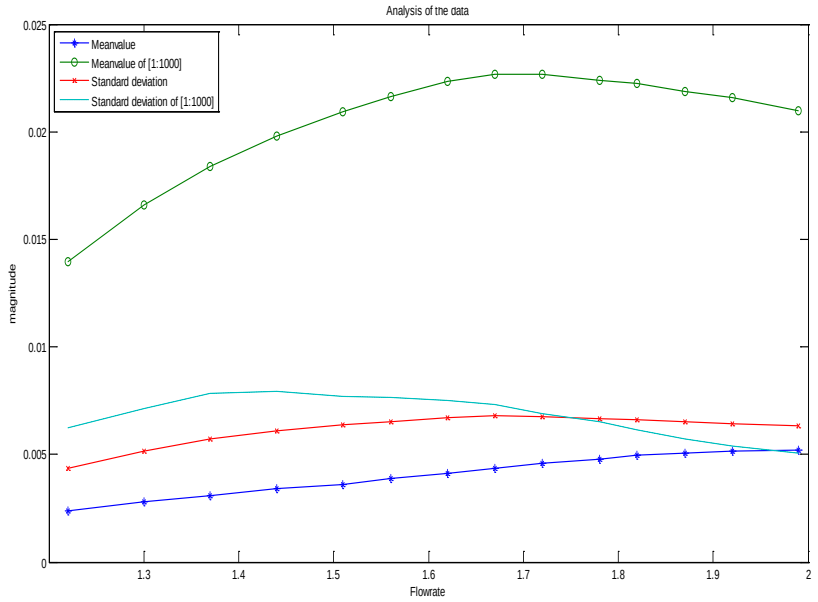


Figure 4.7 Mean value and standard deviation of the data

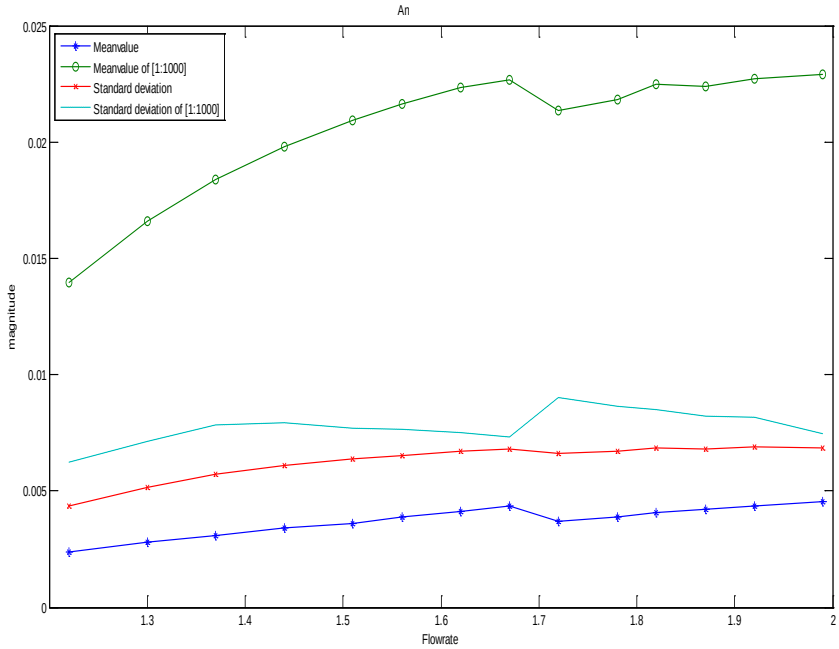


Figure 4.8 Mean value and standard deviation of the data after drying the sensor before the 172 lpm test.

### 4.2.4 Evaluation of Position C

During this test, the microphone was attached in the same horizontal plane as the tip outlet. The distance to the outlet did not need to be very precise, since it would not affect the result, which will be discussed later in this part. The test was conducted 10 times consecutively with flow rates from 1.0 lpm to 1.9 lpm in steps of 0.1 lpm. The frequency response plot was constructed (Fig. 4.9) and then an analysis was made to see if trends in the characteristic of the response were continuous. The general trend for those curves was that the amplitude increased as the flow rate increased.

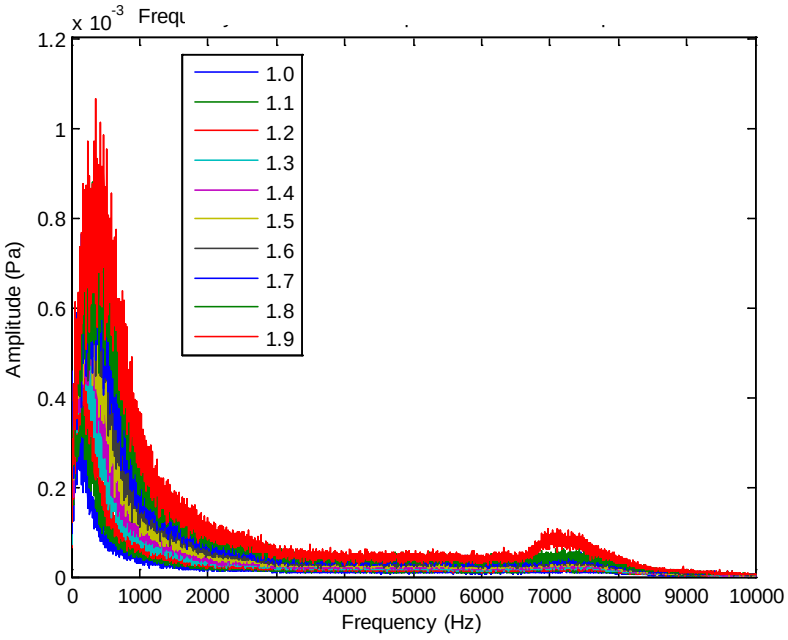


Figure 4.9 Frequency response for consecutive 10 tests

Upon closer evaluation of the spectral responses from 0 Hz to 3000 Hz (Fig. 4.10), it was clear that the amplitude became larger each time and the peak

frequency seems to shift to the right as flow rate increases. This observation will form the core for further investigations of the performance of the sensor discussed in Chapter 5. Also, the average sound pressure level and standard deviataion showed a strong correlation to flow rate (Figs. 4.11, 4.12).

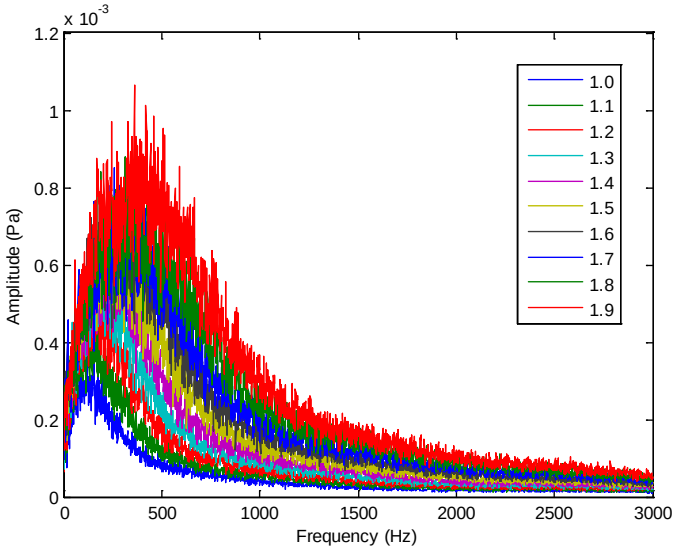


Figure 4.10 Frequency response for consecutive 10 tests in the frequency 3000 Hz

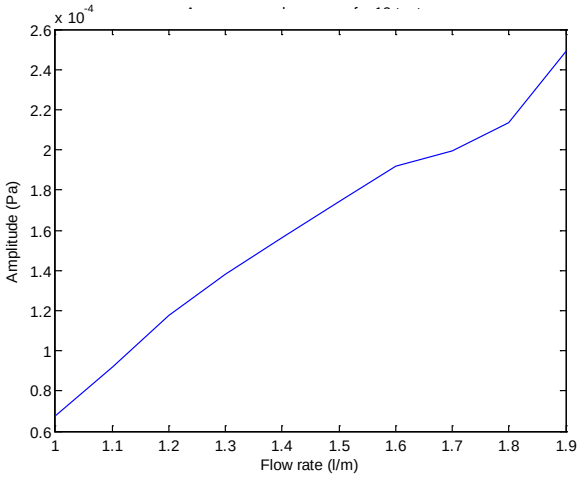


Figure 4.11 Average sound pressure for different flow rates

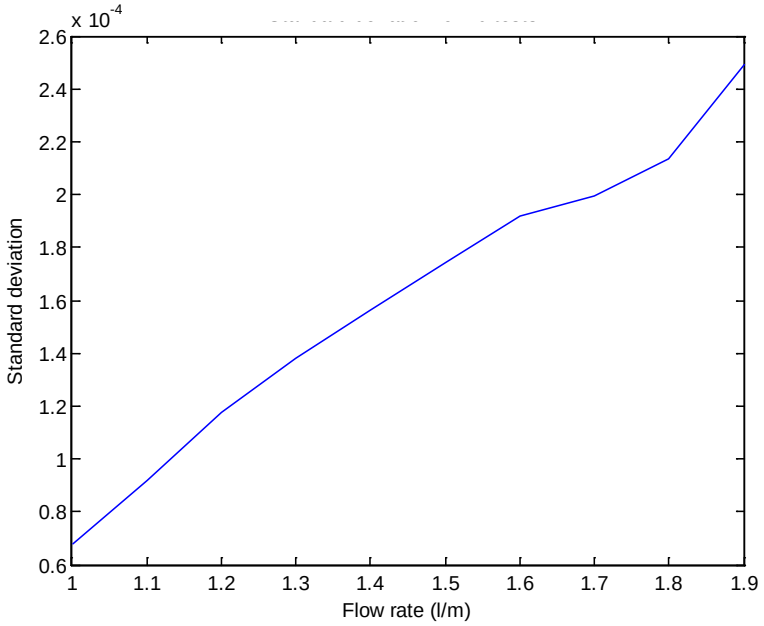


Figure 4.12 Standard deviation for different flow rates

Note that these 10 tests were conducted without any change of the environment, thus the result proved that there would not be a serious impact of the water drops on the microphone over a period of time. The mean value and standard deviation of the amplitude confirmed the continuous trend for the increasing of the flow rate and proved that there was a broad response of flow rate to many characteristics of the signal. It would be easier to pick up one aspect for analysis to distinguish the flow rate.

## 4.3 Summary and Conclusions

In this chapter, three potential locations were tested by the same microphone. For the first one, which was close to the surface of the nozzle, the results showed that there was not an obvious indication of flow rate observed by analyzing the frequency response, and there was too much noise, especially high frequency noise. The second location showed more promise as a test location since it has distinct characteristic for each flow rate but if it was held there for a period, it would be dampened by the water drops. After drying the microphone, it had the same trend as it showed previously. If the microphone were to be used in this location, other protection measures would need to be taken in order to keep the microphone dry. Finally, the location close to the outlet of the nozzle tip was discussed. It showed very good characteristics in every aspect analyzed. The frequency response curve shifted and increased with increasing the flow rate. The standard deviation and average sound power showed an almost linearly dependent correlation with the flow rate in a low frequency range. The result showed that the sensor was not wet after a period of tests. So this position would be a good place for holding the microphone. Thus the location C was chosen for further experimentation.

# Chapter Five: Data Post-Processing

## 5.1 Description

After the best sensor and mounting location were selected, the next task was to perform a more thorough analysis of the performance of the sensor and to find ways to use the sensor to characterize the flow rate through the nozzle. This chapter mainly discusses the analysis of the experimental data.

Figure 5.1 contains an example plot of the frequency domain information for the flow rate ranges from 1.0 lpm to 2.0 lpm. The maximum frequency of the data acquisition board was 50 kHz. Several interesting and potentially useful characteristics of the plot were noted. Distinct peaks were occurring at 500 Hz, 7500 Hz and some other high frequency domains.

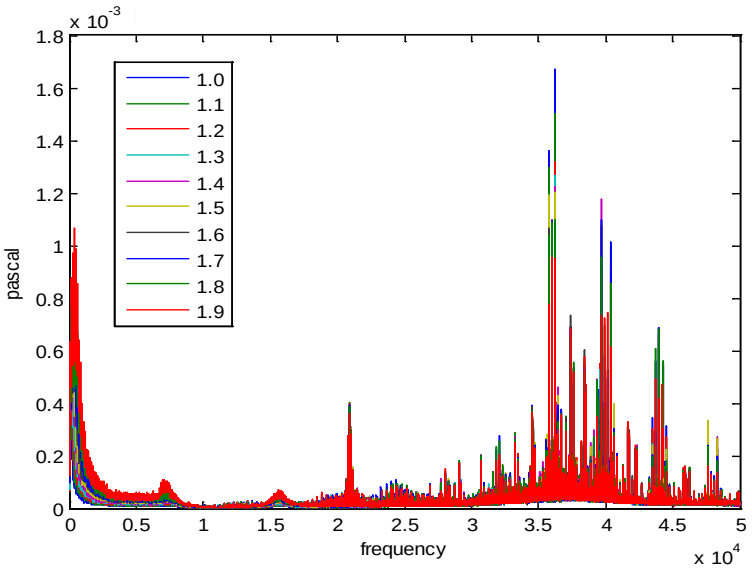


Figure 5.1 Frequency response of acoustic signal for flow rates of 1.0 - 2.0 lpm with the Knowles BL-21994-000 microphone

When zooming in to the frequency range below 7 kHz (Fig. 5.2, 5.3), which is the upper bound for most microphones, it was clear that the amplitude was increasing along with the increase of flow rate and there also seemed to be a shift in the frequency at which the peak occurred. Also there was a consistent impulse noted at 61 Hz, which would impact the curve fitting process. The impulse should be eliminated if it had nothing to do with the flow rate but was caused by power supply interference.

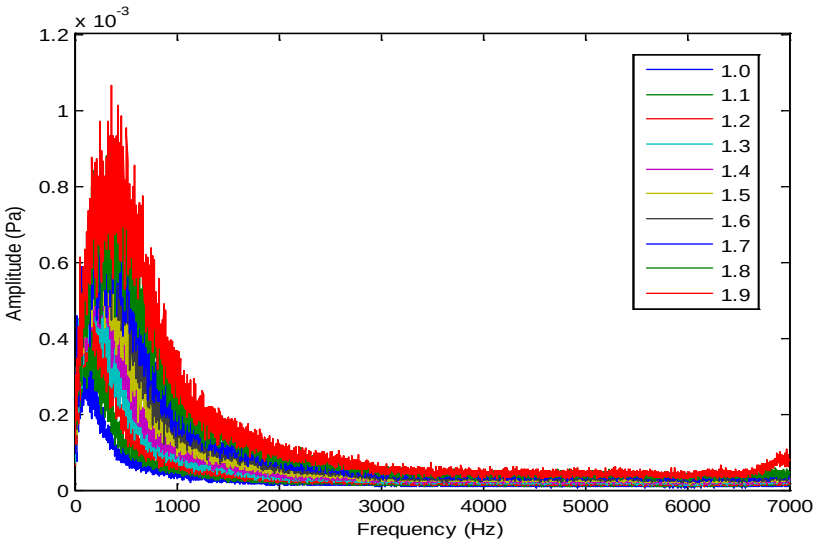


Figure 5.2 Frequency response for flow rate 1.0 - 2.0 lpm within the range 0- 7000 Hz

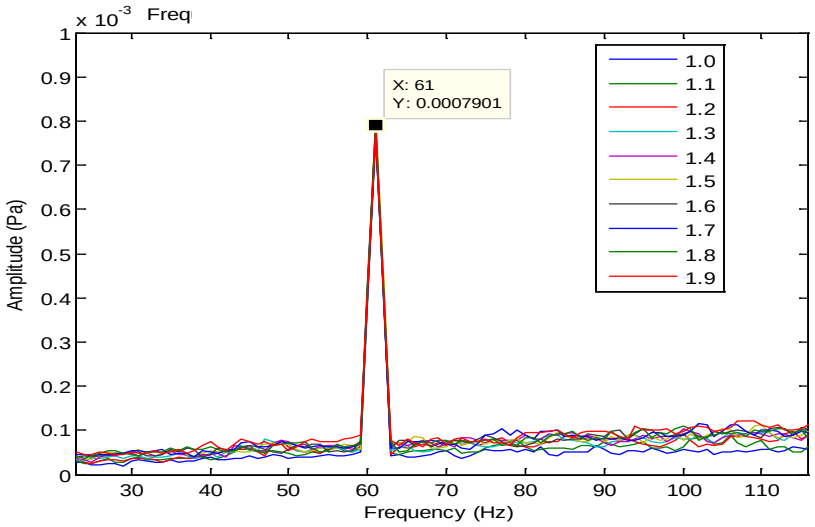


Figure 5.3 Impulse signal occurring at 61 Hz in the frequency response

The following are the specific tasks that were performed to further analyze the acoustic information collected with the microphone:

1. Analyze the data within the whole frequency range from 1 to 50KHz, from the perspective of the trend of the mean value and standard deviation of the amplitude.
2. Analyze the data within the frequency range from 1 to 10KHz, which was the frequency range of the microphone. The trends in the mean value and standard deviation of the amplitude were compared with the results from task 1.
3. Explore the causes of the phonmena that appeared at the frequency of 61 Hz.

4. Analyze the ampiltude of the first major peak that appeared after the 61 Hz anomoly.
5. Analyze the shift of the frequency location of the first major peak.

The following key pieces of equipment were used in the experiments.

*Microphone: Knowles BL-21994, CUI CMP-5247TF-K*
*Software: Matlab, LabVIEW, Microsoft Excel, NI-Max*
*Data Acquisition Board: NI-USB 4431*
*Nozzle tips: MR80-04*

### 5.1.1 Microphone Setup

In this project, two microphone were used: CUI CMP-5247TF-K and Knowles BL-21994. The purpose of using two different microphones was to compare the results. Since the Knowles BL-21994 is of high quality, the results should be relatively precise and reliable, but the CUI CMP-5247TF-K would be more realistic for this application due to its low price. If they give similar results, then the cheaper microphone would be appropriate in this application.

To use the CUI CMP-5247TF-K (Fig. 5.4) a measurement circuit (Fig. 5.5) had to be constructed according to the manufacturer recommendations. The output of this circuit was then connected to the DAQ system.

Figure 5.4 CUI CMP-5247TF-K microphone.

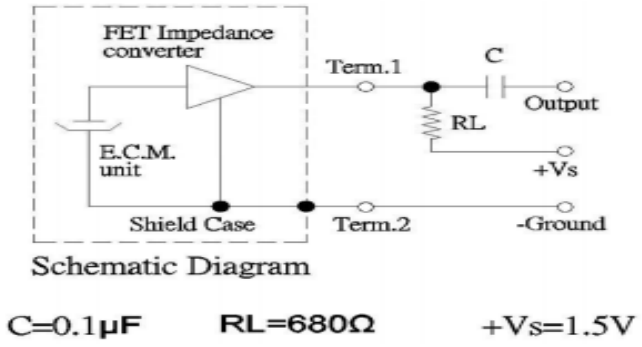


Figure 5.5 Measurement Circuit for CUI CMP-5247TF-K microphone

## 5.2 Data Processing Method Comparison

In 5.1, five potential ways to analyze the data were described. For the first two, the mean value and standard deviation for the frequency ranges of 0-50 KHz and 0-10 KHz were plotted (Figs. 5.6 and 5.7). It was easy to get some information about the amplitude and signal strength with respect to different flow rates.

First was the plot of the frequency range 0-50000 Hz:

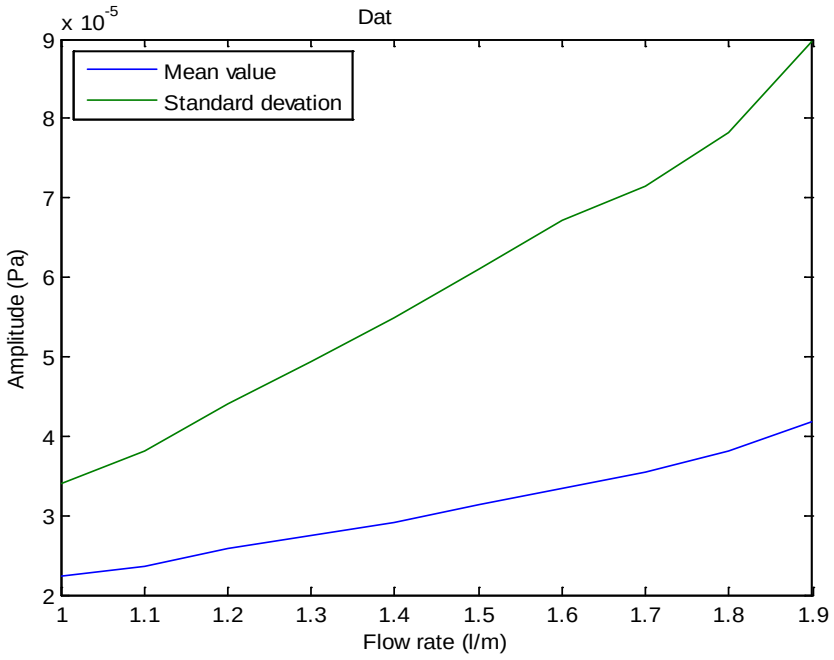


Figure 5.6 Mean value and standard deviation of the frequency response amplitude in the frequency range of 1- 50 KHz

Interestingly, the mean value of amplitude in the whole frequency range was increasing as flow rate increased, which indicated that with the higher flow rate, the avarage sound pressure was larger. That was to be expected. The standard deviation trend showed that when the flow rate got larger, the data points were more spread out, which indicated that the sound pressure on each frequency did not increase with the same trend; some frequencies increased faster than others.

The next task was to analyze the frequency range to 10 kHz since it was microphone's bound for receiving the sound frequency. Also, reducing the analysis range would reduce computing time. The results (Fig. 5.7) revealed a similar trend to the one from the previous analysis. The mean value of

the signal strength had a sharper trend than found in the whole range analysis. This meant that it would be a more distinguishable indicator than sampling the whole frequency range.

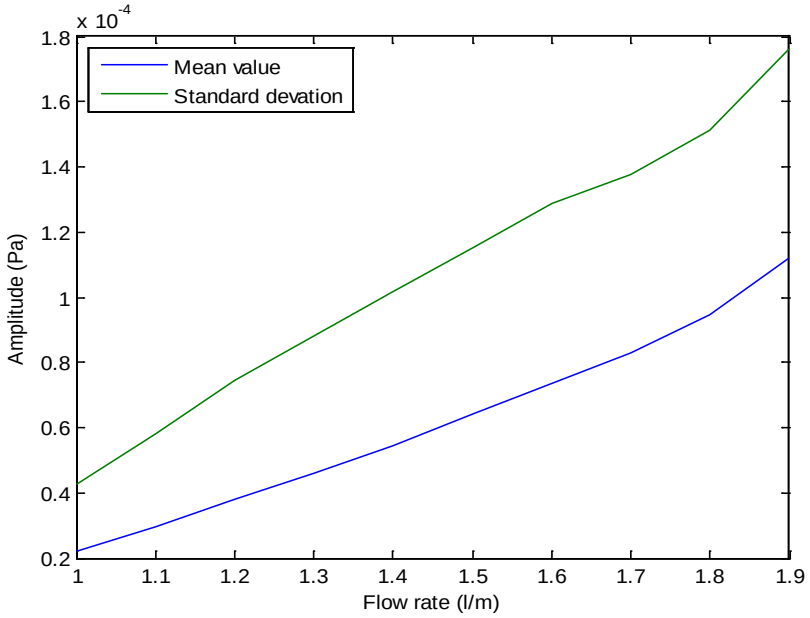


Figure 5.7 Mean value and standard deviation of the frequency response amplitude in the frequency range of 1-10 KHz

From the results above, it was concluded that the mean value or standard deviation could be used as an indicator of flow rate. The concern was that when putting the application into actual field tests, there would be all kinds of unpredictable noise, and it would be hard to know how greatly that would affect the results. Besides, the standard deviation was also an unstable reference standard, because in the farm field, the microphone would detect all kinds of noise which could appear at different frequencies, so it would result in amplitude changes in some freuquency components.

Table 5.1 shows the results of the tests repeated 5 times for the flow rates of 1.0-1.5 lpm within the frequency range 0-10 kHz. In different working enviroments, the meanvalue would shift dramatically, so it would not be a good indication of flow rate.

Table 5.1 Average amplitude for 5 tests of the frequency range 0-10 KHz in Pascals

| Flow Rate (lpm) | Test1($10^{-2}$) | Test2($10^{-2}$) | Test3($10^{-2}$) | Test4($10^{-2}$) | Test5($10^{-2}$) |
|---|---|---|---|---|---|
| 1.0 | 0.0189 | 0.0152 | 0.0176 | 0.0183 | 0.0199 |
| 1.1 | 0.0235 | 0.0224 | 0.0242 | 0.0232 | 0.0211 |
| 1.2 | 0.0287 | 0.0256 | 0.0290 | 0.0296 | 0.0276 |
| 1.3 | 0.0343 | 0.0312 | 0.0332 | 0.0322 | 0.0342 |
| 1.4 | 0.0405 | 0.0389 | 0.0395 | 0.0402 | 0.0412 |
| 1.5 | 0.0495 | 0.0452 | 0.0485 | 0.0473 | 0.0501 |

It was important to get some information from the unique amplitude peak occurring at 61 Hz on all the plots. The first task was to determine if the the amplitude peak had any relationship to flow rate change. If not, it was significant to study the cause of the impulse response. Table 5.2 and Figure 5.8 show the amplitude values at 61 Hz for different flow rates. The correlation of flow rate and amplitude at 61 Hz did not show a clear trend or relation. It showed an irregular trend with the increase of flow rate, which meant that it was not caused by flow.

Table 5.2 The peak amplitude at 61 Hz for flow rates from 1.0 -2.0 lpm

| Flow Rate (lpm) | Peak Frequency(Hz) | Amplitude (Pascal) |
|---|---|---|
| 1 | 61 | 0.007663 |
| 1.1 | 61 | 0.007564 |
| 1.2 | 61 | 0.007614 |
| 1.3 | 61 | 0.007435 |
| 1.4 | 61 | 0.007520 |
| 1.5 | 61 | 0.007597 |
| 1.6 | 61 | 0.007659 |
| 1.7 | 61 | 0.007453 |
| 1.8 | 61 | 0.007261 |
| 1.9 | 61 | 0.007170 |
| 2.0 | 61 | 0.007387 |

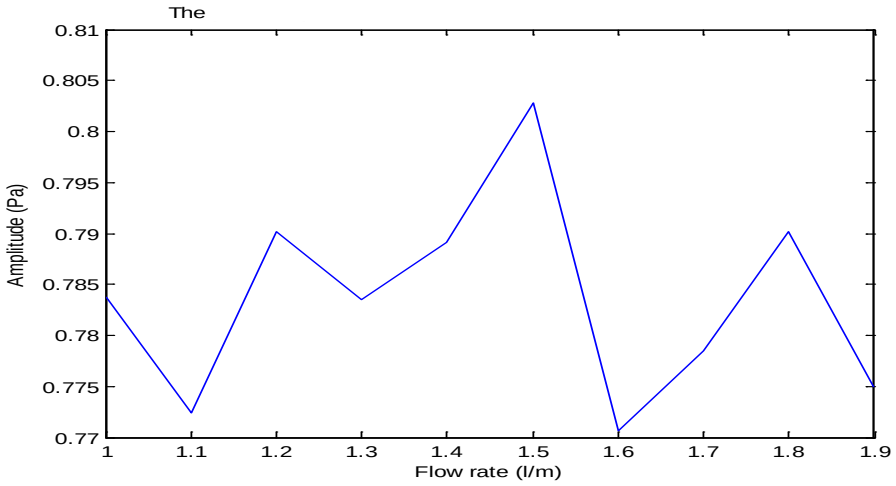


Figure 5.8 The peak amplitude at 61 Hz for flow rates from 1.0 -2.0 lpm

It was still necessary to figure out why there was a impusle happening at 61 Hz. If it was only the exogenous noise, it would be necessary to use some filtering method to remove it from the frequency response to avoid affecting the final results. There were two possible explanations of this strange phenomenon: 1. It was caused by the vibration of pump. Since the microphones were fixed on the boom, the vibration could transmit from the pump to the microphone through the boom. 2. It was casued by power interference. Sixty one hertz is pretty close to 60 Hz, which is the frequency of the AC power supply in US.

To verify the guesses, two tests were conducted with the flow rate at zero but one with the pump running and one with it off. It was clear from the results of two experiments (Fig. 5.9) that the peak occurred whether the pump was turned on or off. In fact, the signal amplitude was stronger when the pump was off, so it was not caused by the interference of the pump vibration. Then it might be caused by power interference. According to the datasheet of the data acquisition borad, a time-varying common-mode voltage was coupled onto the signal of interest, which happens around 60 Hz. There was a high possibility that the sampling information was affected by the AC power supply. Two tests were conducted to confirm this. In these tests, a passive microphone was used. The results showed no power interference (Fig 5.10). This meant that when the AC power supply was not used to provide voltage to microphone, the AC interference was eliminated.

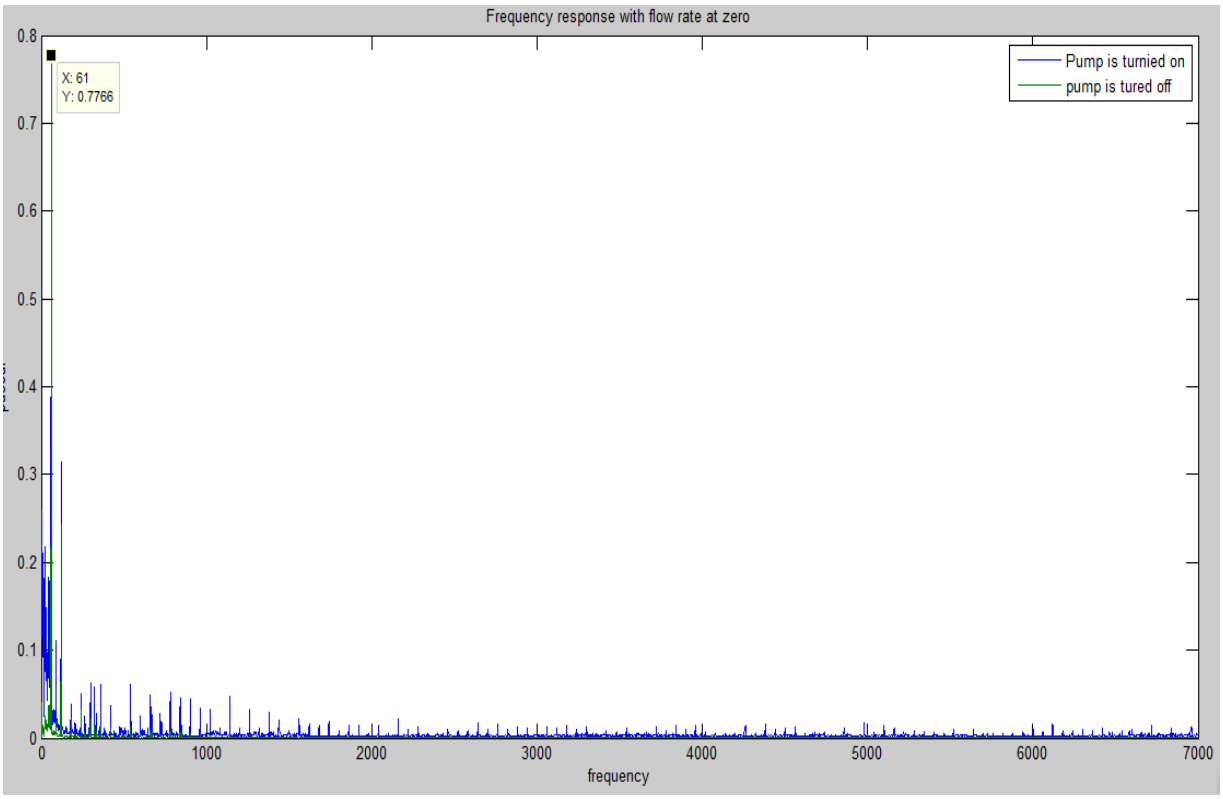


Figure 5.9 Frequency response of two tests at zero flow rate with and without pump running.

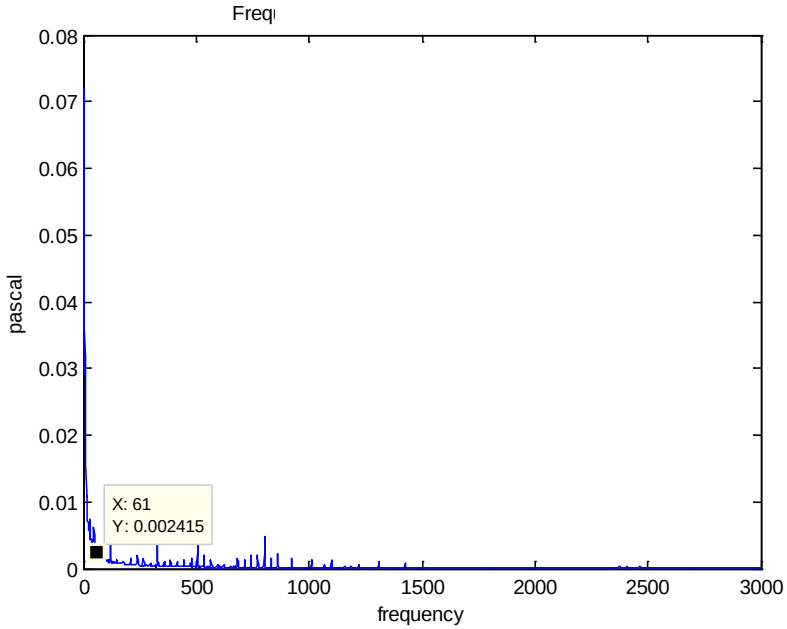


Figure 5.10 Frequency response with a passive microphone at zero flow rate.

The next task was to focus analysis on the first major amplitude peak (Fig. 5.11). The plot showed that for each flow rate it seemed there was a unique peak. Generally speaking, the peak amplitude and frequency shifted as the flow rate increased. As discussed above, the amplitude was not a robust indicator since the amplitude on each frequecy will change with environmental changes or proximity of the microphone. So analyses were to turned to the frequency location of the peak since it was expected to be more robust than other indicators.

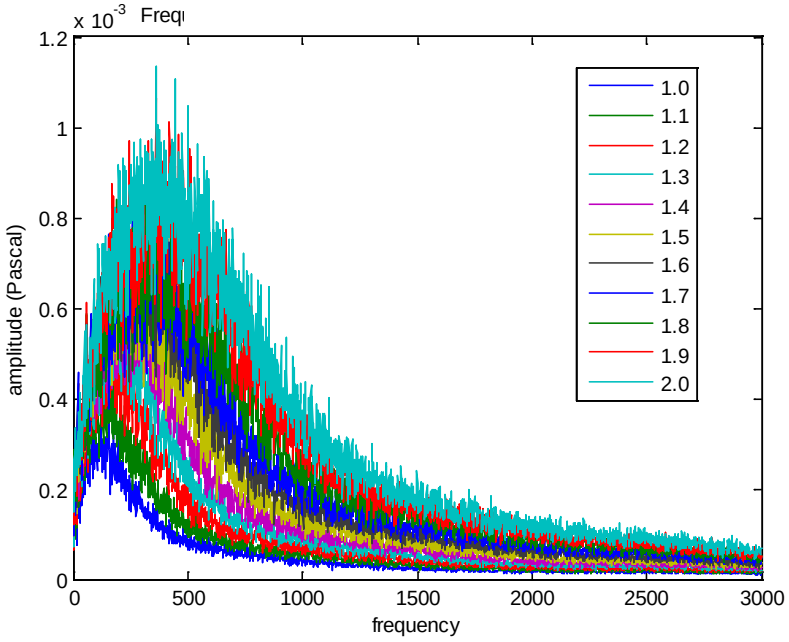


Figure 5.11 Frequency response of the BL-21994-000 microphone for the frequency range 0-3000Hz

## 5.3 Curve Fitting

To reliably describe the frequency response, it was necessary to introduce a curve fitting method to smooth and fit the data. After smoothing the plot, it would be easy to recognize the peak frequencies and compare them. There are three general ways to fit the curves: least square fit, nonlinear fit and smoothing curve fit. Least squares is intended to minimize the square of the error between the original data and the predicted data from the equation, and it is simple and well understood. There are several methods in least squares fit: linear, polynomial, power and Guassian. Nonlinear fit is also called Nonlinear regression fit. Typically, machine learning methods are used for non parametric regression. Three ways are provided for nonlinear regression: Gauss-Newton algorithm, gradient descent algorithm and Levenberg-Marquardt algorithm. Smoothing curve fit differs from the other two methods in that it does not give a determined function because it is used when there is not an equation to represent the curve. There are several ways to do the smoothing curve: cubic spline, interpolate and weighted (KaileidaGraph. *Curve Fitting Guide*). In this project, since a determined equation was ultimately desirable, the last catergory was not utilized. Usually, calculation by hand to get the a good curve fit is really hard and impractical. The **cftool** curve and surface fitting tool in Matlab was utilized. **Cftool** had a variety of models to choose from to find a good fit. To use **cftool**, one could use the cftool command with other inputs or just directly type cftool. It would automatically open the cftool menu once the program ran to that step. After opening the cftool, the original x and y data should be inputted, which in this case were the frequency range in Hz (x) and the corresponding amplitude in Pascals

(y). Then the operator could choose different options in the menu, such as smooth, fitting or analysis. Through trial and error two models were applied generally to describe and represent the frequency response curve: polynomial and Gaussian.

The polynomial model was:

$$p(x) = \sum_{i=1}^{N} p_i x^{i-1} \tag{5.1}$$

which was the combination of different orders of x, where the N was associated with the highest order that one wants to estimate. In Matlab, the highest order could be 9, thus N was 10. A good point of using polynomial as the fitting model for this project was that it would skip outlier points that were far away from the data.

The Gaussian Model was:

$$y = \sum_{i=1}^{n} a_i e^{[-(\frac{x-b_i}{c_i})^2]} \tag{5.2}$$

which was the combination of different sin and cos waves. In this equation, $a_i$ was the amplitude, $b$ was the centroid (location), $c$ was related to the peak width, and $n$ was the number of peaks to fit, where in Matlab, $1 \leq n \leq 8$.

The following goals were set for the analysis:

1. The fitted curve should show a good estimation of the original curve, and the contact ratio should be relatively high.

2. The error between original data and predictions should be as small as possible.
3. The computing time should be as small as possible, since in real application it will be implemented as a real time process using some kind of embedded processor.
4. Each fitted curve should have distinct characteristics that indicate the flow rate, and it should be robust.

The results of the analysis would determine: 1. which model should be used, 2. which order to use, and 3. what frequency range is good for analysis.

### 5.3.1 Gaussian Model Fitting

First, a Gaussian model was tried on the original curves. The Gaussian model is widely applied in different engineering fields. The highest order of the Gaussian model was $8^{th}$ order, thus it was not hard to match the curve with different orders to see which one was the best.

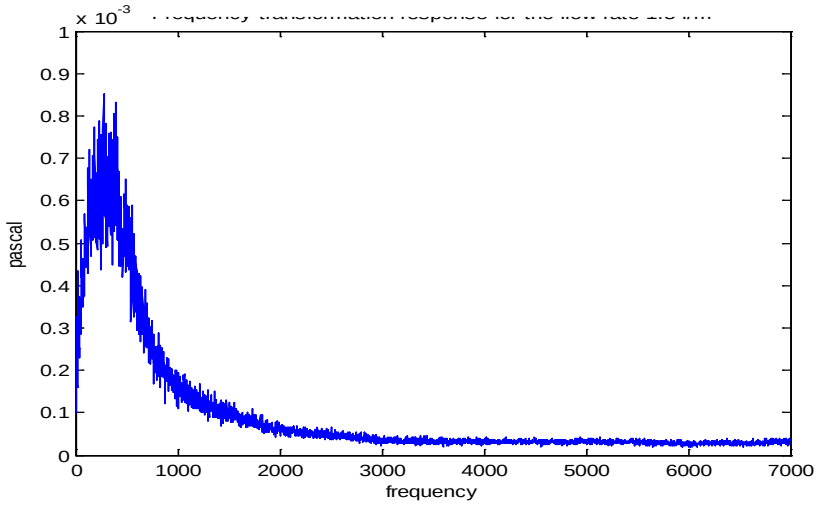


Figure 5.12 Frequency response plot at a flow rate of 1.5 lpm

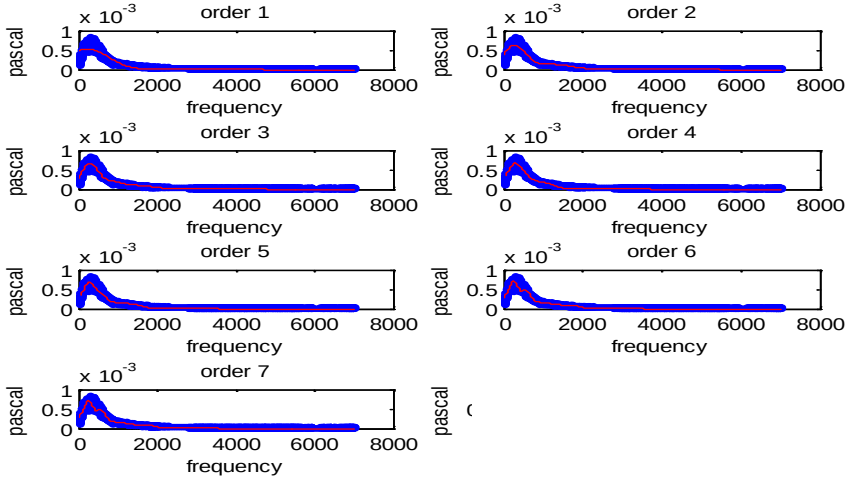


Figure 5.13 Gaussian model fitting with order 1-8 for the flow rate 1.5 lpm

The results of the fitted curves using orders from 1-8 for a flow rate of 1.5 lpm with the frequency range 0-7000 Hz (Figs. 5.12, 5.13) showed that when the order was below 5, the algorithm gave a smooth curve but it did not show a good representation of the original data. When the order increased, the curves were

more close to the original data but the it showed more irregularity near the peak frequency, which resulted in not being able to determine a robust, distinguishable value. In order to determine whether the Gaussian Model could be practiced in this case, an 8$^{th}$ order model for the flow rates from 1.0-1.7 lpm for the frequency range 0-3000 Hz was tried (Fig. 5.14).

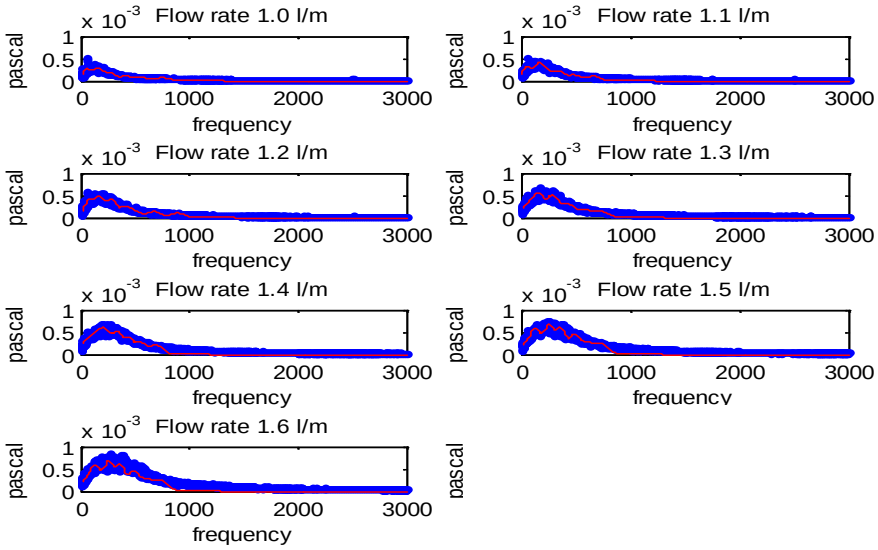


Figure 5.14 Gaussian model fitting with order 8 for the flow rate 1.0 -1.7 lpm

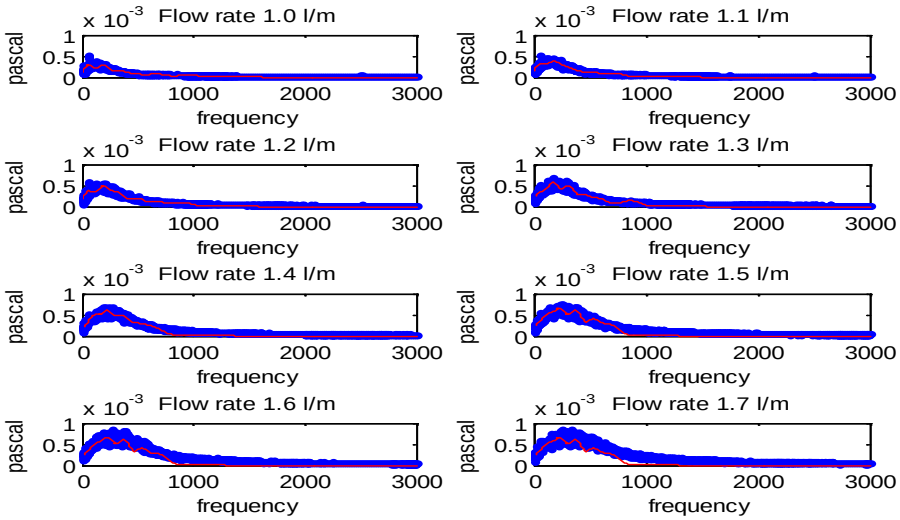


Figure 5.15 Gaussian model fitting with order 6 for the flow rate 1.0 -1.7 lpm

When a 6$^{th}$ order Gaussian model was tried (Fig. 5.15), it still showed that the noise affected the result in low flow rate. So it was necessary to smooth the original data and not consider the noise peak that occurred at 61 Hz into the fitting process. However, considering that the application was real time processing, it would increase the computation time. Thus by using Gaussian Model, there would be a tradeoff between curve fitting precision and processing time. It was hard to abandon either because it was necessary to have precision to predict the flow rate in a very short period. Thus the next step was to move to a Polynomial Model to see if it would better help since it would automatically omit noise.

### 5.3.2 Polynomial Model Fitting

The next step was to try a polynomial model. The frequency range considered first was 0-7 kHz (Fig. 5.16, 5.17). It was easy to see that the fitted curve should be greater than a second order polynomial.

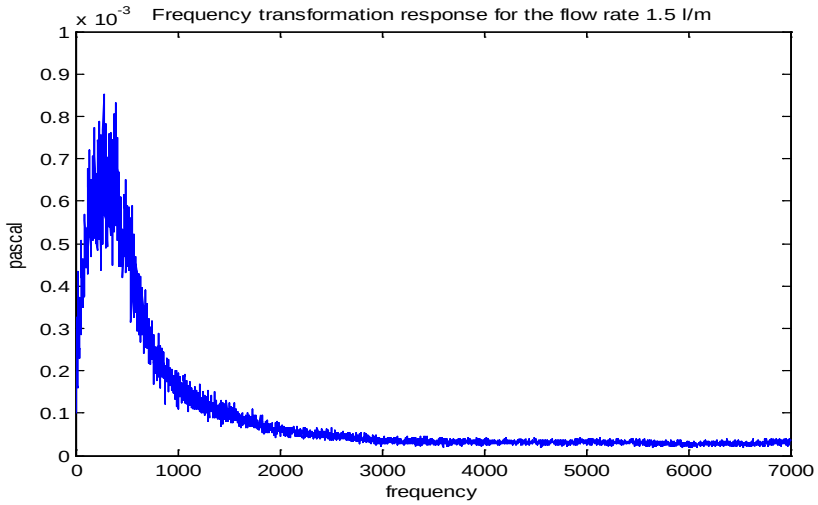


Figure 5.16 Frequency response plot at the flow rate 1.5 lpm

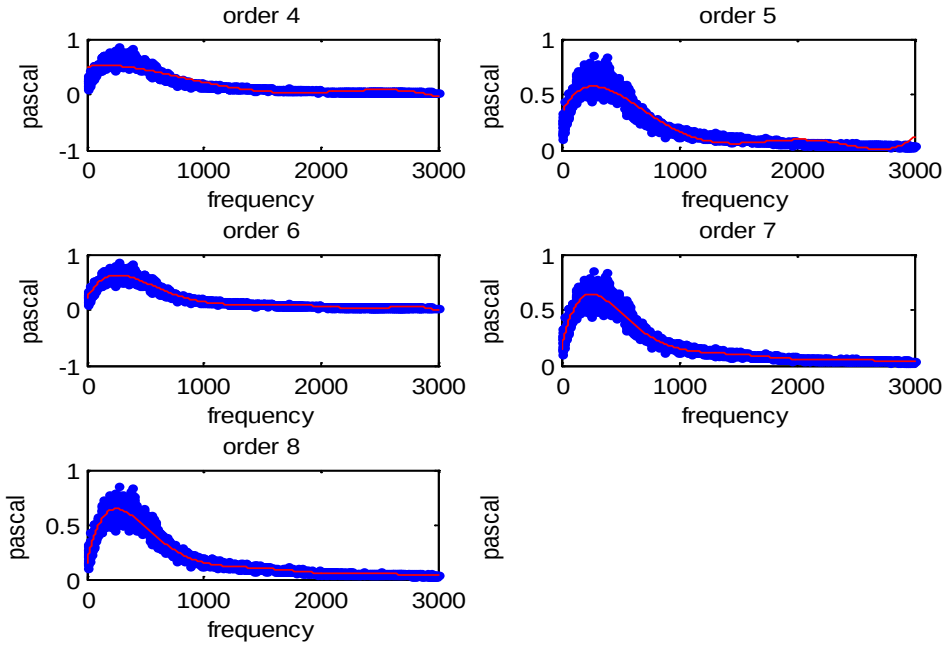


Figure 5.17 Polynomial model fitting with order 4-8 for the flow rate 1.5 lpm

The best polynomial models for the frequency range 0-7 kHz were 7th order, 8th order and 9th order. One possible reason for the necessity of such a high order was that the frequency range chosen was inapproporiate. When narrower frequency ranges of 0-1 kHz, 0- 2 kHz and 0- 3 kHz were considered (Fig 5.18, Fig 5.19 and Fig 5.20), the fit was much better with lower order polynomials. Note that the smaller frequency range would require much less processing time.

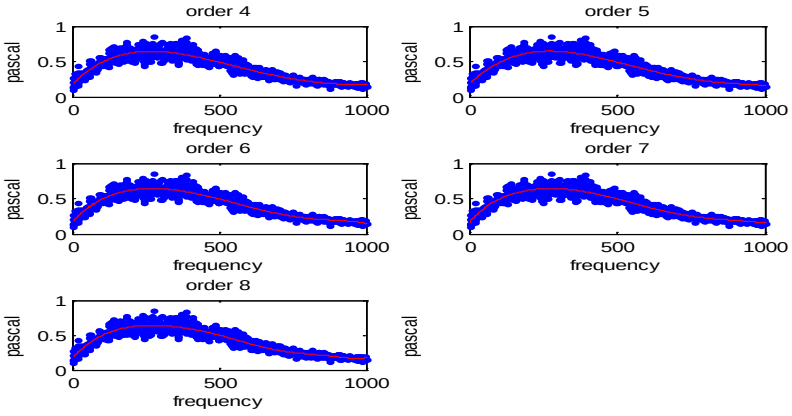


Figure 5.18 Polynomial model fitting with order 4-8 for the flow rate 1.5 lpm with the frequency range 0-1000 Hz

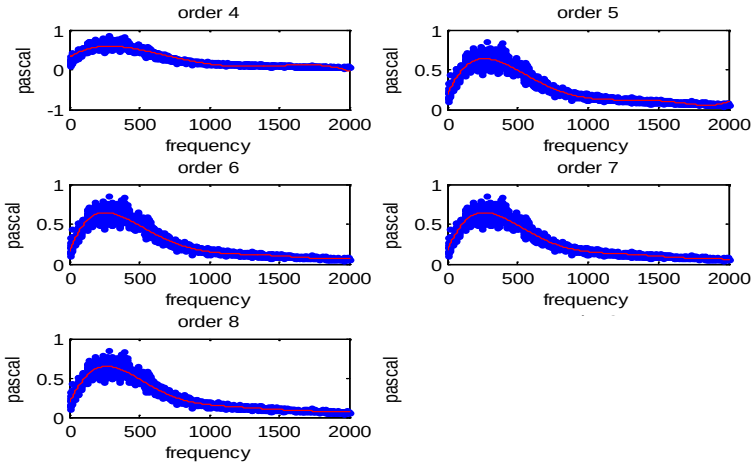


Figure 5.19 Polynomial model fitting with order 4-8 for the flow rate 1.5 lpm with the frequency range 0-2000 Hz

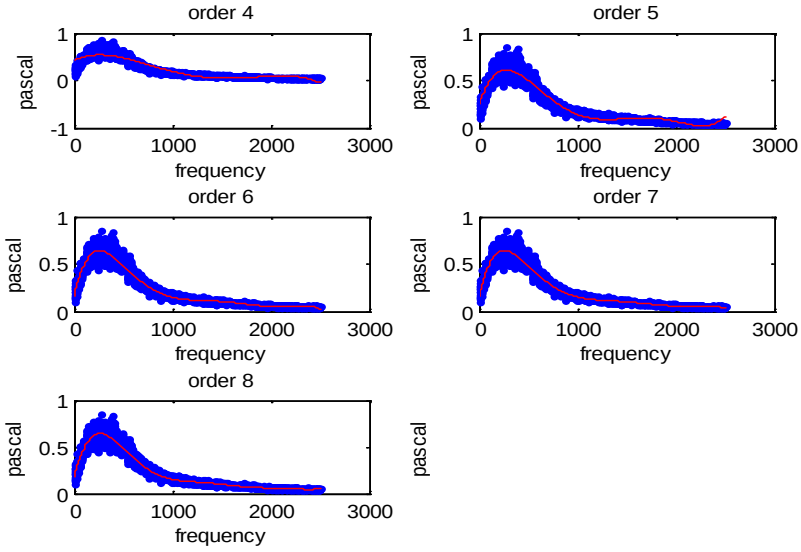


Figure 5.20 Polynomial model fitting with order 4-8 for the flow rate 1.5 lpm with the frequency range 0-2500 Hz

The 3 selected frequency ranges showed that analyzing the data within 2000 Hz should be accurate since within that range, the results on each order were

good. After a successive calculation and comparison, 2500 Hz was chosen as the final analysis frequency range.

Five tests were conducted on 5 different days with the same flow rate range from 1.0 lpm to 2.0 lpm in 0.1-lpm intervals. Two microphones were used in these experiments: BL-21994-000 and CUI CMP-5247TF-K. They were fixed at the same place to receive signals at the same time. After collecting data for 5 different tests, the frequency analysis range was varied (0-1500 Hz, 0-2000 Hz, 0-2500 Hz, 0-3000 Hz) to determine which was the most approporiate.

Tables 5.3-5.6 and Figures 5.21-5.28 showed the peak frequency for different tests with the two microphone (Note in the following discussion that BL represents the more expensive BL-21994-000 microphone, and CUI represents the cheaper CUI CMP-5247TF-K.)

Table 5.3 Comparison of the peak frequency for 5 tests with the frequency range 0-1500 Hz for both microphones.

| Flow | 1st Test | | 2nd Test | | 3rd Test | | 4th Test | | 5th Test | |
|---|---|---|---|---|---|---|---|---|---|---|
| Rate(lpm) | BL | CUI | BL | CUI | BL | CUI | BL | CUI | BL | CUI |
| 1 | 115 | 96 | 112 | 94 | 115 | 95 | 110 | 94 | 113 | 94 |
| 1.1 | 138 | 110 | 138 | 111 | 134 | 109 | 134 | 109 | 133 | 109 |
| 1.2 | 159 | 129 | 157 | 126 | 153 | 127 | 161 | 131 | 160 | 130 |
| 1.3 | 184 | 152 | 178 | 152 | 177 | 148 | 189 | 162 | 186 | 161 |
| 1.4 | 202 | 176 | 200 | 176 | 203 | 181 | 195 | 167 | 201 | 180 |
| 1.5 | 220 | 202 | 235 | 234 | 233 | 218 | 229 | 219 | 223 | 211 |
| 1.6 | 250 | 270 | 255 | 272 | 255 | 271 | 256 | 272 | 250 | 267 |
| 1.7 | 288 | 317 | 284 | 306 | 277 | 312 | 288 | 317 | 302 | 325 |
| 1.8 | 318 | 345 | 318 | 345 | 308 | 338 | 294 | 331 | 316 | 345 |
| 1.9 | 331 | 352 | 349 | 368 | 351 | 367 | 356 | 371 | 352 | 369 |
| 2 | 378 | 386 | 380 | 384 | 379 | 385 | 369 | 380 | 345 | 371 |

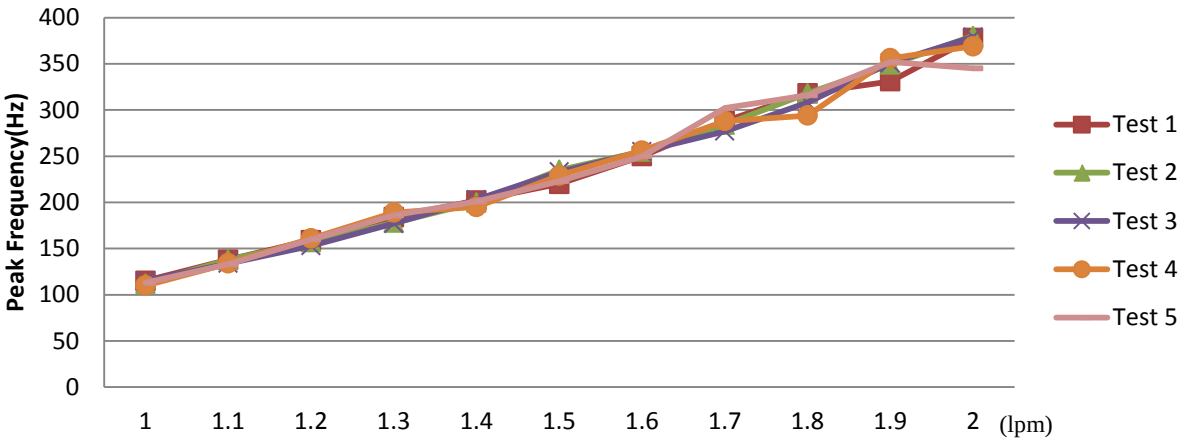


Figure 5.21 Peak frequency vs flow rate for 5 tests with the BL microphone.

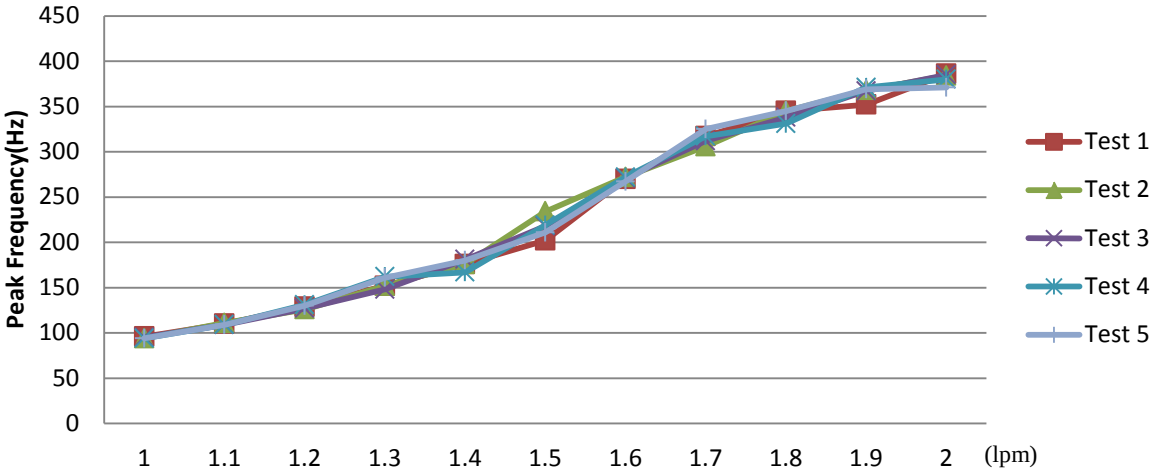


Figure 5.22 Peak frequency vs flow rate for the 5 tests with the CUI microphone.

Table 5.4 Comparison of the peak frequency for 5 tests with the frequency range 0-2000 Hz for two microphones

| Flow | 1st Test | | 2nd Test | | 3rd Test | | 4th Test | | 5th Test | |
|---|---|---|---|---|---|---|---|---|---|---|
| Rate(lpm) | BL | CUI | BL | CUI | BL | CUI | BL | CUI | BL | CUI |
| 1 | 112 | 108 | 111 | 107 | 112 | 108 | 110 | 107 | 111 | 107 |
| 1.1 | 131 | 122 | 131 | 122 | 129 | 121 | 129 | 121 | 127 | 120 |
| 1.2 | 153 | 139 | 151 | 137 | 147 | 137 | 153 | 140 | 154 | 141 |
| 1.3 | 180 | 162 | 174 | 160 | 173 | 158 | 186 | 170 | 182 | 167 |
| 1.4 | 201 | 184 | 200 | 185 | 202 | 187 | 195 | 179 | 201 | 186 |
| 1.5 | 219 | 203 | 232 | 218 | 230 | 212 | 226 | 211 | 222 | 208 |
| 1.6 | 247 | 236 | 251 | 240 | 249 | 236 | 254 | 244 | 250 | 239 |
| 1.7 | 283 | 275 | 283 | 271 | 276 | 269 | 287 | 277 | 289 | 277 |
| 1.8 | 312 | 308 | 309 | 303 | 310 | 305 | 297 | 292 | 313 | 306 |
| 1.9 | 340 | 329 | 345 | 340 | 346 | 339 | 348 | 344 | 347 | 344 |
| 2 | 368 | 375 | 368 | 377 | 369 | 379 | 361 | 370 | 348 | 350 |

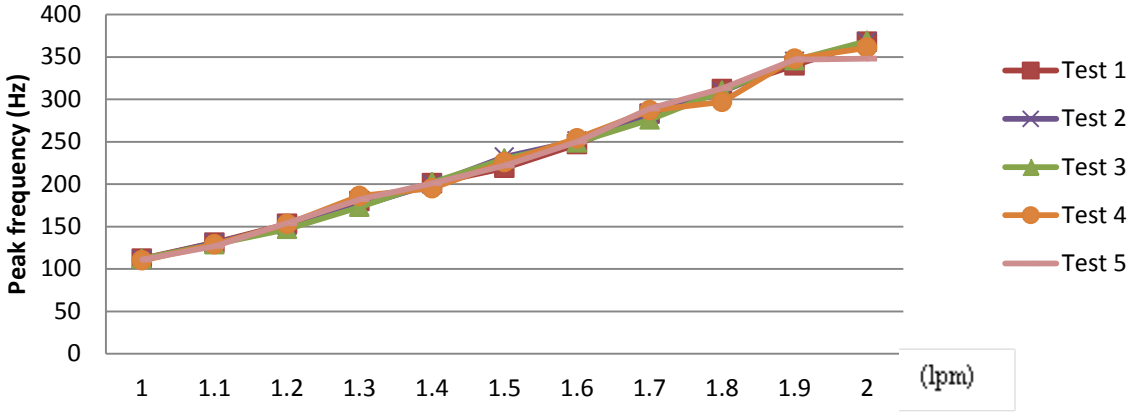


Figure 5.23 Peak frequency vs flow rate for the 5 tests with BL microphone.

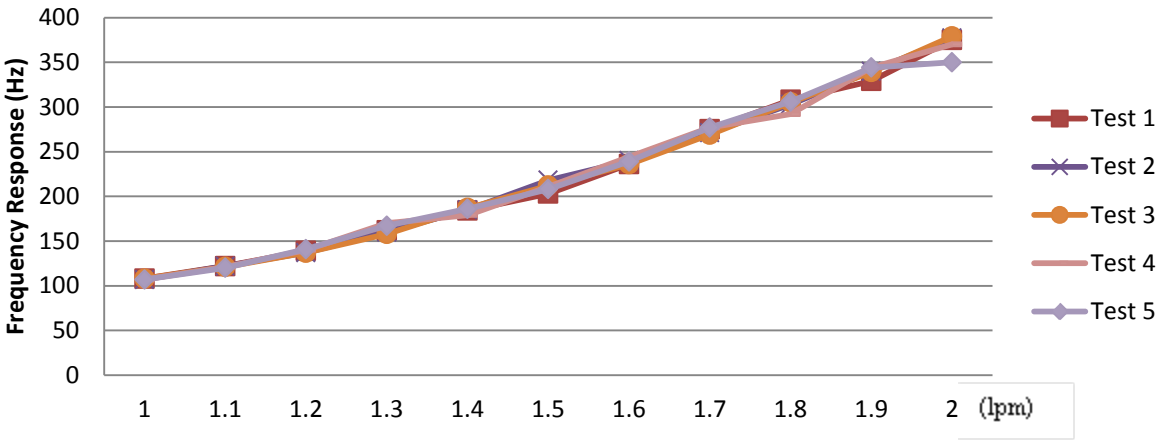


Figure 5.24 Peak frequency vs flow rate for the 5 tests with CUI microphone.

Table 5.5 Comparison of the peak frequency for 5 tests with the frequency range 0-2500 Hz for two microphones

| Flow Rate(lpm) | 1st Test | | 2nd Test | | 3rd Test | | 4th Test | | 5th Test | |
|---|---|---|---|---|---|---|---|---|---|---|
| | BL | CUI | BL | CUI | BL | CUI | BL | CUI | BL | CUI |
| 1 | 115 | 118 | 115 | 116 | 115 | 117 | 114 | 116 | 115 | 116 |
| 1.1 | 131 | 131 | 132 | 131 | 131 | 131 | 131 | 131 | 130 | 129 |
| 1.2 | 149 | 146 | 148 | 145 | 146 | 144 | 149 | 146 | 151 | 147 |
| 1.3 | 173 | 165 | 168 | 163 | 168 | 163 | 176 | 171 | 173 | 169 |
| 1.4 | 194 | 186 | 194 | 187 | 195 | 189 | 191 | 184 | 195 | 188 |
| 1.5 | 218 | 210 | 228 | 220 | 226 | 214 | 225 | 216 | 220 | 212 |
| 1.6 | 247 | 240 | 251 | 242 | 249 | 239 | 253 | 244 | 250 | 242 |
| 1.7 | 282 | 272 | 283 | 270 | 275 | 267 | 284 | 273 | 285 | 274 |
| 1.8 | 308 | 299 | 303 | 293 | 306 | 296 | 293 | 285 | 306 | 295 |
| 1.9 | 328 | 314 | 331 | 320 | 340 | 326 | 339 | 325 | 336 | 327 |
| 2 | 369 | 348 | 367 | 350 | 366 | 346 | 363 | 343 | 346 | 335 |

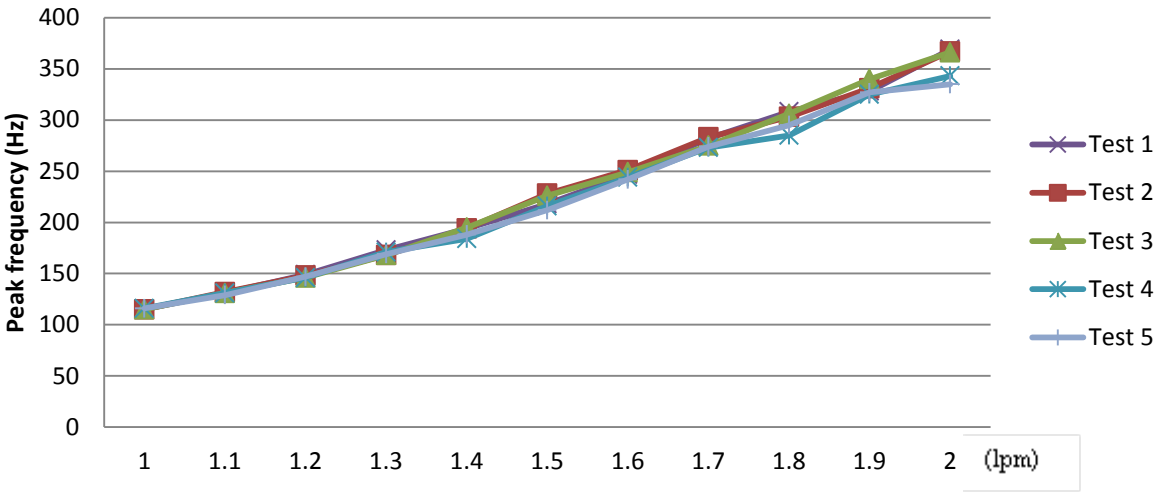


Figure 5.25 Peak frequency vs flow rate for the 5 tests with the microphone Knowles BL-21994-000

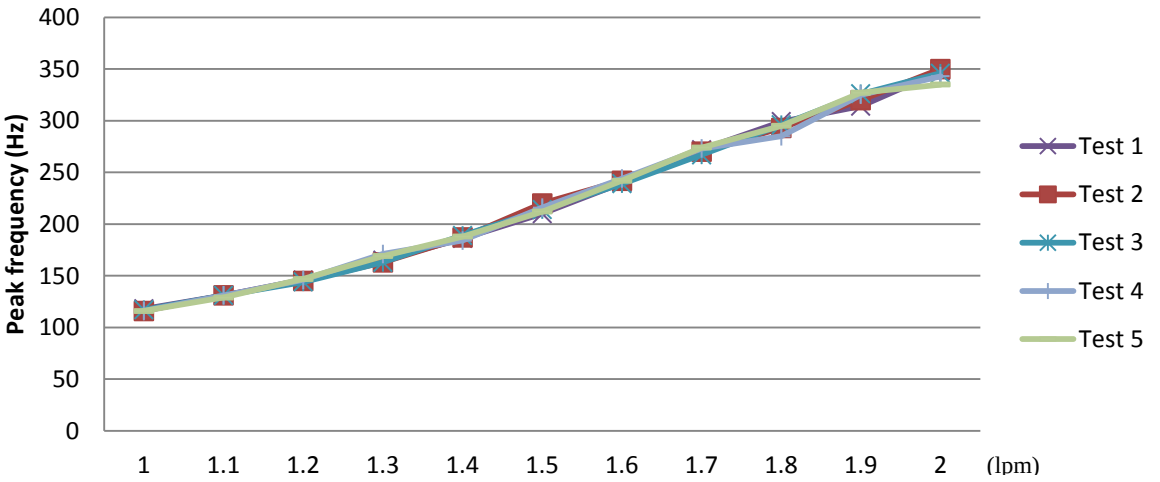


Figure 5.26 Peak frequency vs flow rate for the 5 tests with the microphone CUI CMP-5247TF-K

Table 5.6 Comparison of the peak frequency for 5 tests with the frequency range 0-3000 Hz for two microphones

| Flow Rate(lpm) | 1st Test | | 2nd Test | | 3rd Test | | 4th Test | | 5th Test | |
|---|---|---|---|---|---|---|---|---|---|---|
| | BL | CUI | BL | CUI | BL | CUI | BL | CUI | BL | CUI |
| 1 | 119 | 123 | 118 | 121 | 119 | 122 | 117 | 121 | 118 | 121 |
| 1.1 | 136 | 138 | 136 | 138 | 136 | 138 | 136 | 138 | 135 | 137 |
| 1.2 | 153 | 153 | 152 | 152 | 150 | 152 | 153 | 153 | 154 | 154 |
| 1.3 | 172 | 169 | 169 | 168 | 169 | 168 | 173 | 173 | 173 | 172 |
| 1.4 | 190 | 187 | 190 | 188 | 192 | 189 | 188 | 186 | 191 | 188 |
| 1.5 | 214 | 209 | 220 | 215 | 219 | 211 | 219 | 214 | 215 | 210 |
| 1.6 | 244 | 238 | 245 | 239 | 244 | 237 | 247 | 240 | 246 | 240 |
| 1.7 | 280 | 271 | 281 | 269 | 275 | 268 | 282 | 272 | 285 | 273 |
| 1.8 | 308 | 299 | 303 | 293 | 306 | 296 | 297 | 288 | 307 | 296 |
| 1.9 | 328 | 314 | 330 | 320 | 339 | 325 | 338 | 325 | 335 | 326 |
| 2 | 363 | 345 | 362 | 348 | 360 | 344 | 358 | 342 | 343 | 334 |

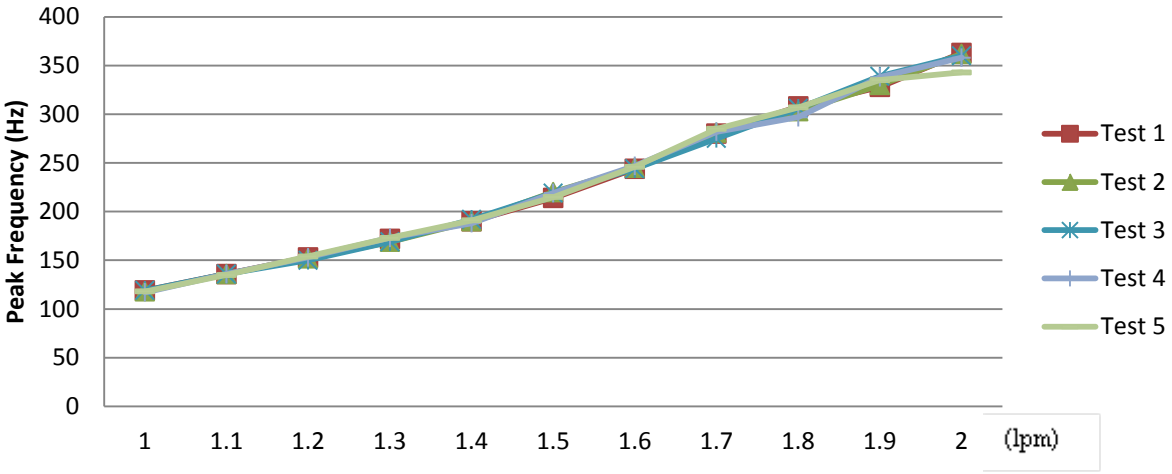


Figure 5.27 Peak frequency vs flow rate for the 5 tests with the microphone Knowles BL-21994-000

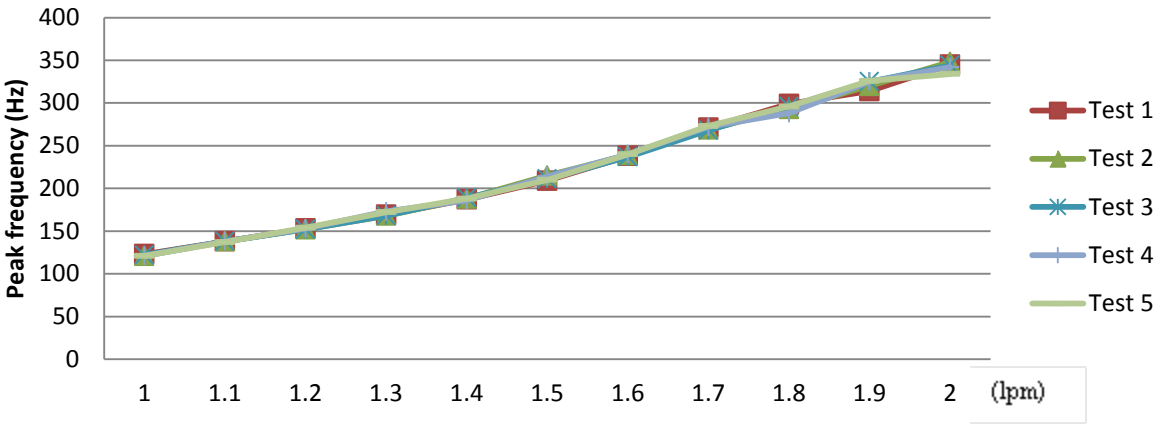


Figure 5.28 Peak frequency vs flow rate for 5 tests with the microphone CUI CMP-5247TF-K

When comparing the four choices of frequency ranges that were tested, 2500 Hz performed the best. When the range was increased to 3000 Hz, there was little difference in the peak frequency curve relative to the 0- 2500 Hz range, so based on the repeated tests, the 0- 2500 Hz was chosen as our frequency analysis range.

As discussed earlier, it was interesting to see that both microphones had a pretty close result for different flow rates. The intervals between each flow rate were very close. Both of the peak frequency curves show the same linear trend with the flow rate.

## 5.4 Impact of different locations

In chapter four, the position of the microphone was chosen so that the sensor would be fixed near the nozzle outlet within the same horizontal plane. Then a question arose about the proximity of the microphone to the nozzle.

Would the distance between the nozzle tip and the microphone affect the sensor performance?

Then several tests were performed to verify if the distance had an impact on the results. Three distances were chosen: 1.0 cm, 1.5 cm, 2.0 cm. At each distance, four different flow rates were evaluated: 1.0, 1.2, 1.4, 1.8 lpm.

Table 5.7 shows the peak frequency with the chosen method for the tested flow rates. From the table it was apparent that the peak frequency shifted downward when the distance increased. In other words, the further the sensor was from the nozzle tip, the lower peak frequency. According to Stroke's Law, in the same medium that sound propagates, higher frequencies will attenuate faster than lower frequency, which could explain this interesting phenomenon. Thus in future tests, the location should be stated since it affects the result so much.

Table 5.7 Frequency of peak amplitude for different distances between microphone and nozzle (Hz)

| Flow Rate (lpm) | 1.0 cm | 1.5 cm | 2.0 cm |
|---|---|---|---|
| 1.0 | 169 | 122 | 111 |
| 1.2 | 176 | 163 | 149 |
| 1.4 | 220 | 197 | 176 |
| 1.6 | 271 | 252 | 226 |

Table 5.8 Peak amplitude for different distances between microphone and nozzle (Pa)

| Flow Rate (lpm) | 1.0 cm | 1.5 cm | 2.0 cm |
|---|---|---|---|
| 1.0 | 0.5712 | 0.3112 | 0.2787 |
| 1.2 | 0.6432 | 0.5306 | 0.4139 |
| 1.4 | 0.7463 | 0.6237 | 0.4708 |
| 1.6 | 0.8190 | 0.7339 | 0.5982 |

## 5.5 Summary and Conclusions

The tests described in this chapter were aimed at determining a specific fitting method to use to get a precise and smooth fitted curve. By using curve fitting, the peak frequency value and/or the peak frequency range to distinguish each flow rate was discovered.

In the first part, several ways to analyze the original data in the frequency domain were discussed such as the mean value and standard deviation in certain frequency range. The conclusion was that the first major amplitude peak would be a good indication of flow rate since it would be robust regardless of different environments.

After deciding what value would be critical, two main fitting methods were compared : Gaussian and Polynomial model. By analyzing the fitted curves, the polynomial model was found to be better. The Gaussian model could help better explain the theoretical background of the experiments but it didn't give a

smooth and robust curve. The polynomial model could provide a better match to the original curve and it gave a distinguishable value for different flow rates. In this situation, a $9^{th}$ order polynomial model was chosen to analyze the frequency range of 0- 2500 Hz as the principle method to indicate flow rate.

At the end of this part, the impact of the distance to the nozzle was discussed and verified by Stroke's Law. The nearer the sensor was located, the higher the peak frequency; thus, in the future analyses the precise location should be stated.

# Chapter Six: Additional Experiments

## 6.1 Description

The previous tests and results reported in this study were focused on one singular nozzle tip, specifically the MR 80-04 Combo-Jet nozzle tip manufactured by Wilger, Inc., Lexington, TN. The analyses of the acoustic signal showed good stability for indicating flow rate through the nozzle. The next task was to determine if the relationships developed in the study would extend to other nozzle tips commonly used on the machinery.

First, it is necessary to introduce the nozzle tip family produced by Wilger, Inc. since this test was conducted using their nozzle tips. The MR in the previous experiment represented the droplet size spectra that it would generate. In the Wilger Combo-Jet nozzle family, there were 4 kinds of nozzle tips that produced different droplet size: DR, ER, MR, SR. Farmers could choose one of them according to their needs. The number 80 indicates that the spray pattern will exit the nozzle in a plane that is 80 degrees wide. Then the number 04 is an indication of the size of the nozzle and by association the expected flow rate at a given pressure. To evaluate the robustness of the relationships developed for the MR 80 04 nozzle, a set of nozzles from within this family were selected. Specifically, tests were conducted with MR 80 04, MR 80 06, and MR 80 08 to determine the effects of nozzle size. Then additional tests were conducted with MR 80 04, SR 80 04, DR 80 04, and ER 80 04 to evaluate the effects of different droplet size spectra.

## 6.2 MR 80 Series results

### 6.2.1 Experiment results for MR 80- 04

The MR 80-04 was the smallest nozzle used in this application. Recommendation of operating pressure limits for this nozzle was 1.5 BAR to 7.0 BAR and the corresponding flow rate was expected to be 1.13 lpm to 2.07 lpm. So in this case, the flow rates chosen to be analyzed ranged from 1.0 lpm to 2.1 lpm in 0.1 lpm intervals.

Table 6.1 contains a list of the test and data processing conditions. Table 6.2 shows the results for 5 repeated tests. Table 6.3 shows the statistical analysis results for the experimental data. Then it was easy to plot the statistical trend for the MR 80-04 against flow rate. The plot represented the average of 30 repeated experiments as is the case for all the following experiments.

Table 6.1 Test and analysis conditions for MR 80-04

| | |
|---|---|
| Microphone | CUI CMP-5247TF-K |
| Distance (cm) | 1.5 |
| Sampling frequency (Hz) | 100k |
| Analysis frequency range (Hz) | 2500 |
| Fitting model | Polynomial Model |
| Model order | 9 |

Table 6.2 Location of the amplitude peak of 30 repeated tests on MR 80-04

| Flow rate (lpm) | 1st Test (Hz) | 2nd Test (Hz) | 3rd Test (Hz) | 4th Test (Hz) | 5th Test (Hz) |
|---|---|---|---|---|---|
| 1 | 136 | 140 | 137 | 139 | 139 |
| 1.1 | 150 | 148 | 149 | 148 | 149 |
| 1.2 | 160 | 159 | 160 | 158 | 161 |
| 1.3 | 179 | 173 | 175 | 178 | 178 |
| 1.4 | 199 | 192 | 196 | 197 | 194 |
| 1.5 | 224 | 222 | 222 | 221 | 221 |
| 1.6 | 246 | 248 | 245 | 247 | 246 |
| 1.7 | 286 | 279 | 286 | 287 | 284 |
| 1.8 | 326 | 315 | 324 | 323 | 318 |
| 1.9 | 350 | 355 | 350 | 348 | 355 |
| 2 | 390 | 386 | 388 | 393 | 397 |
| 2.1 | 427 | 427 | 428 | 429 | 424 |

Table 6.3 Analysis of the average peak frequency and the concentration of the data

| Flow rate (lpm) | 1 | 1.1 | 1.2 | 1.3 | 1.4 | 1.5 | 1.6 | 1.7 | 1.8 | 1.9 | 2 | 2.1 |
|---|---|---|---|---|---|---|---|---|---|---|---|---|
| Average (lpm) | 138.2 | 148.8 | 159.6 | 176.6 | 195.6 | 222 | 246.4 | 284.4 | 321.2 | 351.6 | 390.8 | 427 |
| STD | 1.469 | 0.748 | 1.019 | 2.244 | 2.416 | 1.095 | 1.019 | 2.870 | 4.069 | 2.870 | 3.867 | 1.673 |

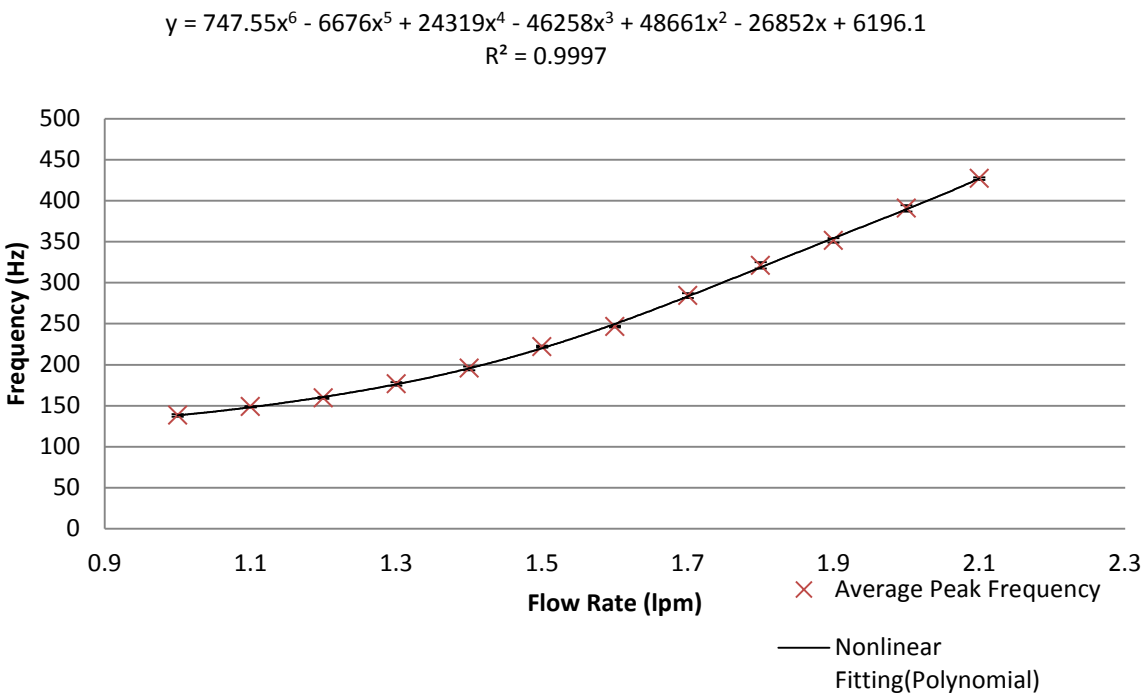


Fig 6.1 Model of the trend of the peak frequency of MR 80-04(with error bars)

### 6.2.2 Experiment result for MR 80- 06

The MR 80-06 was the next nozzle tested. Recommendation of operating pressure limits for this nozzle was 1.5 BAR to 5.0 BAR and the corresponding flow rate was expected to be 1.7 lpm to 3.1 lpm. So in this case, the flow rate that chosen to be analyzed ranged from 1.7 lpm to 3.1 lpm in 0.1 lpm intervals.

Table 6.4 shows the test and data processing condition. Table 6.5 shows the results for 5 repeated tests Table 6.6 was the analysis results for the experimental data for this nozzle. After discovering the average values and standard deviations, the next step was to plot the statistical trend (Fig 6.2).

Table 6.4 Test and analysis condition for MR 80-06

| | |
|---|---|
| Microphone | CUI CMP-5247TF-K |
| Distance (cm) | 1.5 |
| Sampling frequency (Hz) | 100k |
| Analysis frequency range (Hz) | 2500 |
| Fitting model | Polynomial Model |
| Model order | 9 |

Table 6.5 Location of the amplitude peak of 30 repeated tests for MR 80-06

| Flow rate (lpm) | 1st Test (Hz) | 2nd Test (Hz) | 3rd Test (Hz) | 4th Test (Hz) | 5th Test (Hz) |
|---|---|---|---|---|---|
| 1.8 | 139 | 137 | 133 | 138 | 134 |
| 1.9 | 147 | 146 | 148 | 147 | 144 |
| 2 | 157 | 160 | 156 | 158 | 160 |
| 2.1 | 169 | 170 | 170 | 169 | 170 |
| 2.2 | 181 | 183 | 182 | 180 | 183 |
| 2.3 | 198 | 194 | 198 | 195 | 195 |
| 2.4 | 203 | 202 | 203 | 201 | 203 |
| 2.5 | 217 | 214 | 219 | 215 | 219 |
| 2.6 | 240 | 238 | 238 | 238 | 236 |
| 2.7 | 254 | 258 | 259 | 255 | 256 |
| 2.8 | 263 | 266 | 268 | 270 | 271 |
| 2.9 | 288 | 288 | 292 | 288 | 288 |
| 3.0 | 316 | 317 | 319 | 320 | 314 |
| 3.1 | 340 | 343 | 345 | 342 | 341 |

Table 6.6 Analysis of the average peak frequency and the concentration of the data

| Flow rate (lpm) | 1.8 | 1.9 | 2 | 2.1 | 2.2 | 2.3 | 2.4 | 2.5 | 2.6 | 2.7 | 2.8 | 2.9 | 3 | 3.1 |
|---|---|---|---|---|---|---|---|---|---|---|---|---|---|---|
| Average (lpm) | 136.2 | 146.4 | 158.2 | 169.6 | 181.8 | 196 | 202.4 | 216.8 | 238 | 256.4 | 267.6 | 288.8 | 317.2 | 342.2 |
| STD | 2.31 | 1.35 | 1.6 | 0.48 | 1.16 | 1.67 | 0.8 | 2.03 | 1.26 | 1.85 | 2.87 | 1.6 | 2.13 | 1.72 |

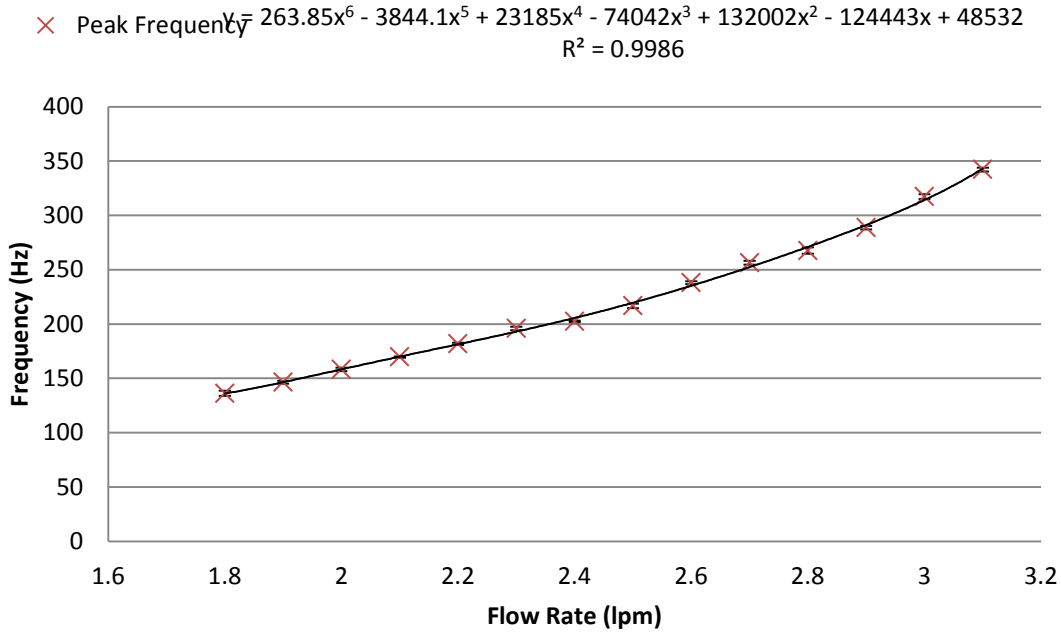


Fig 6.2 Model of the trend of the peak frequency of MR80-06(with error bars)

### 6.2.3 Experiment result for MR 80- 08

The MR 80-08 was the next nozzle to be tested. Recommendation of operating pressure limits for this nozzle was 1.5 BAR to 5.0 BAR and the corresponding flow rate was expected to be 2.26 lpm to 4.13 lpm. So in this case,

the flow rate that chosen to be analyzed ranged from 2.2 lpm to 4.2 lpm in 0.2 lpm intervals.

As discovered in the previous chapter, the best analysis frequency range was 0- 2500 Hz. But for MR 80-08 and MR 80-10, the acoustic vibration caused by the starting flow rate was very tiny, so the 2500 Hz range was too big to analyze (Fig. 6.3). Thus by computation as in chapter 5, it was better to use a frequency range of 0- 1500 Hz for MR 80- 08 and MR 80-10 nozzles (Fig. 6.4).

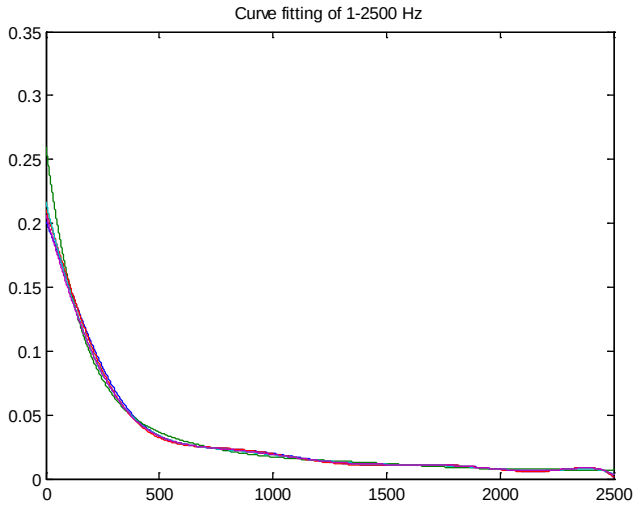


Fig 6.3 Fitting for Frequency response within range 0- 2500 Hz of flow rate 2.2 lpm

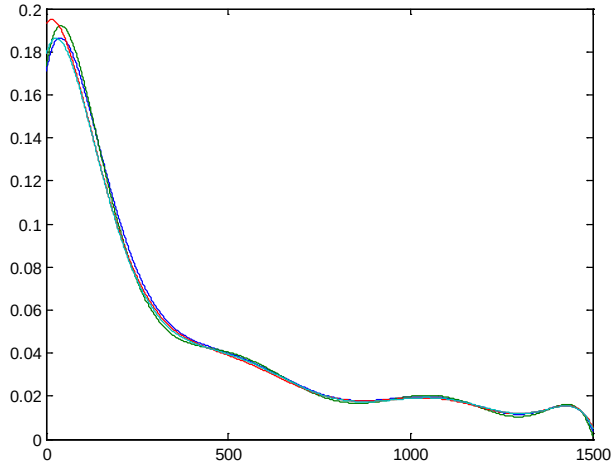


Fig 6.4 Fitting for Frequency response within range 0- 1500 Hz of flow rate 2.2 lpm

Table 6.7 contains a list of the test and data processing condition, Table 6.8 shows the results for 5 repeated tests.

Table 6.7 Test and analysis condition for MR 80-08

| | |
|---|---|
| Microphone | CUI CMP-5247TF-K |
| Distance (cm) | 1.5 |
| Sampling frequency (Hz) | 100k |
| Analysis frequency range (Hz) | 1500 |
| Fitting model | Polynomial Model |
| Model order | 9 |

Table 6.8 Location of the amplitude peak of five repeated tests results for MR 80-08

| Flow rate (lpm) | 1st Test (Hz) | 2nd Test (Hz) | 3rd Test (Hz) | 4th Test (Hz) | 5th Test (Hz) |
|---|---|---|---|---|---|
| 2.4 | 80 | 81 | 81 | 82 | 82 |
| 2.6 | 96 | 91 | 91 | 92 | 96 |
| 2.8 | 108 | 105 | 105 | 104 | 103 |
| 3.0 | 117 | 117 | 116 | 117 | 117 |
| 3.2 | 125 | 126 | 124 | 127 | 129 |
| 3.4 | 144 | 145 | 143 | 141 | 145 |
| 3.6 | 170 | 166 | 171 | 169 | 166 |
| 3.8 | 188 | 189 | 189 | 182 | 192 |
| 4.0 | 212 | 208 | 204 | 207 | 205 |
| 4.2 | 225 | 226 | 232 | 228 | 231 |

Table 6.9 Analysis of the average peak frequency and the concentration of the data

| Flow rate (lpm) | 2.4 | 2.6 | 2.8 | 3 | 3.2 | 3.4 | 3.6 | 3.8 | 4 | 4.2 |
|---|---|---|---|---|---|---|---|---|---|---|
| Average (lpm) | 81.2 | 93.2 | 105 | 116.8 | 126.2 | 143.6 | 168.4 | 188 | 207.2 | 228.4 |
| STD | 0.748 | 2.3151 | 1.673 | 0.4 | 1.7204 | 1.4966 | 2.0591 | 3.2863 | 2.7856 | 2.7276 |

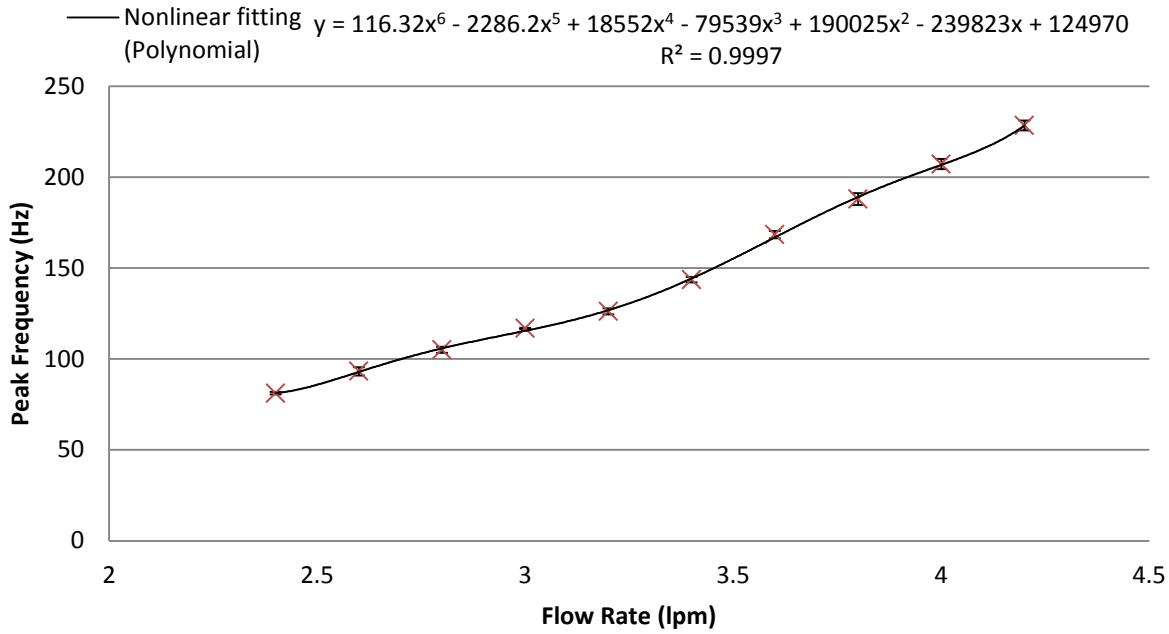


Fig 6.5 Model of the trend of the peak frequency of MR 80-08(with error bars)

### 6.2.4 Experiment result for MR 80- 10

The MR 80-10 was the biggest nozzle that was tested. Recommendation of operating pressure limits for this nozzle was 1.5 BAR to5.0 BAR and the corresponding flow rate was expected to be 1.5 lpm to 5 lpm. So in this case, the flow rate that chosen to be analyzed ranged from 1.0 lpm to 2.1 lpm in 0.1 lpm intervals.

As analyzed in the previous chapter, the frequency range of 1500 Hz was still useful to this type of nozzle. Figures 6.6 and 6.7 showed the analysis with 0-2500 Hz and 0- 1500 Hz for a flow rate of 2.2 lpm. The plot in Figure 6.7 was

more smooth and notable than the plot in Figure 6.6. Thus the frequency range 0-1500 Hz was used for analyses.

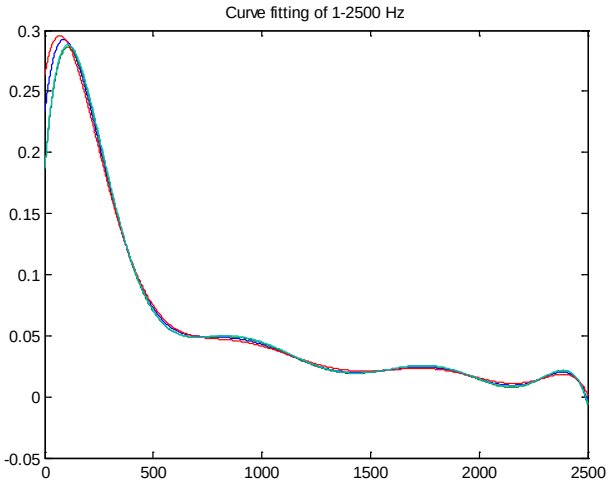


Fig 6.6 Fitting for Frequency response within range 0- 2500 Hz of flow rate 2.8 lpm

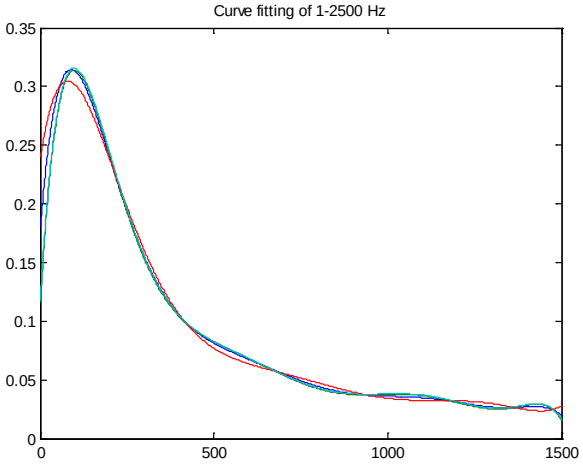


Fig 6.7 Fitting for Frequency response within range 0- 1500 Hz of flow rate 2.8 lpm

Table 6.10 shows the test and data processing condition: Table 6.11 shows the results for 30 repeated tests.

Table 6.10 Test and analysis condition for MR 80-10

| | |
|---|---|
| Microphone | CUI CMP-5247TF-K |
| Distance (cm) | 1.5 |
| Sampling frequency (Hz) | 100k |
| Analysis frequency range (Hz) | 1500 |
| Fitting model | Polynomial Model |
| Model order | 9 |

Table 6.11 Location of the amplitude peak of 30 repeated tests results for MR 80-10

| Flow rate (lpm) | 1st Test (Hz) | 2nd Test (Hz) | 3rd Test (Hz) | 4th Test (Hz) | 5th Test (Hz) |
|---|---|---|---|---|---|
| 2.8 | 66 | 66 | 67 | 64 | 67 |
| 3.0 | 79 | 79 | 79 | 79 | 77 |
| 3.2 | 85 | 83 | 85 | 87 | 86 |
| 3.4 | 86 | 86 | 92 | 87 | 91 |
| 3.6 | 96 | 99 | 104 | 103 | 103 |
| 3.8 | 115 | 113 | 112 | 113 | 115 |
| 4.0 | 120 | 122 | 119 | 122 | 127 |
| 4.2 | 137 | 138 | 136 | 134 | 138 |
| 4.4 | 150 | 145 | 153 | 151 | 147 |
| 4.6 | 165 | 167 | 166 | 164 | 163 |
| 4.8 | 187 | 184 | 181 | 180 | 176 |
| 5.0 | 201 | 198 | 197 | 196 | 199 |
| 5.2 | 219 | 212 | 218 | 223 | 220 |

Table 6.12 Analysis of the average peak frequency and the concentration of the data

| Flow rate (lpm) | 2.8 | 3 | 3.2 | 3.4 | 3.6 | 3.8 | 4 | 4.2 | 4.4 | 4.6 | 4.8 | 5 | 5.2 |
|---|---|---|---|---|---|---|---|---|---|---|---|---|---|
| Average (lpm) | 66 | 78.6 | 85.2 | 88.4 | 101 | 113.6 | 122 | 136.6 | 149.2 | 165 | 181.6 | 198.2 | 218.4 |
| STD | 1.095 | 0.8 | 1.32 | 2.487 | 3.033 | 1.2 | 2.756 | 1.4966 | 2.8565 | 1.414 | 3.720 | 1.7204 | 3.611 |

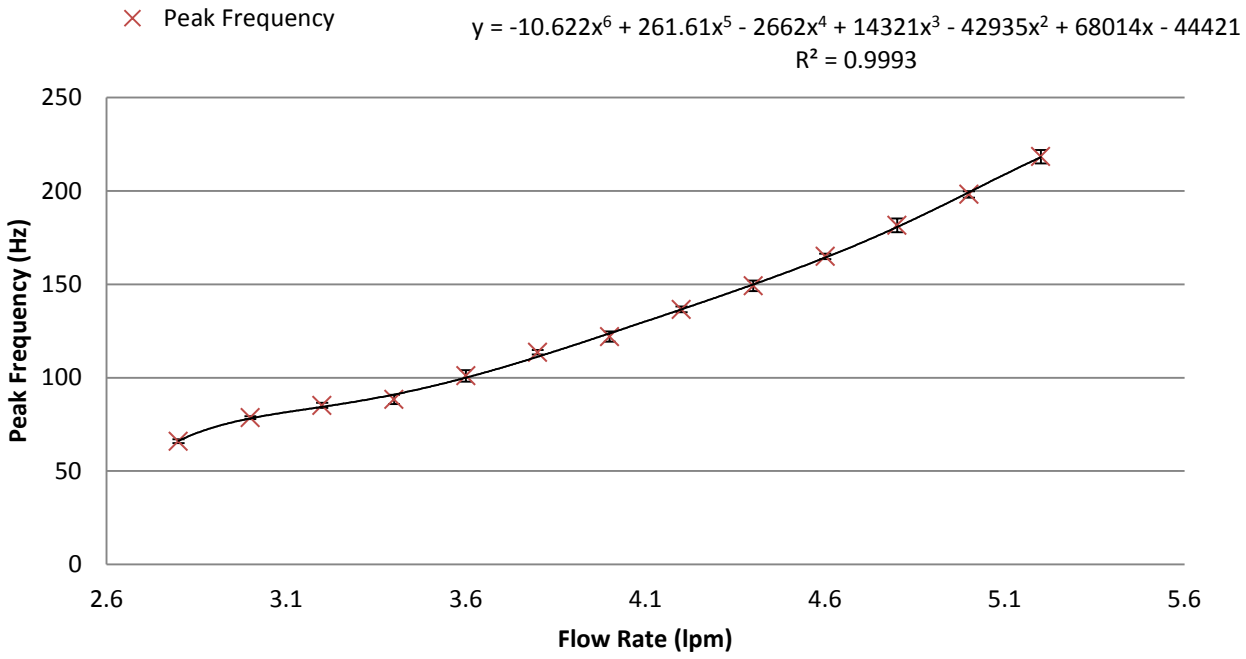


Fig 6.8 Model of the trend of the peak frequency of MR 80-10(with error bars)

## 6.3 ER 80 Series results

### 6.3.1 ER 80-04

The ER 80-04 was the smallest nozzle among selected ones in the ER 80 series. The tested flow rate was from 1.0 lpm to 2.0 lpm with 0.1 lpm interval.

Table 6.13 shows the test and data processing condition, Table 6.14 shows the results for 30 repeated tests.

Table 6.13 Test and analysis condition for ER 80-04

| | |
|---|---|
| Microphone | CUI CMP-5247TF-K |
| Distance (cm) | 1.5 |
| Sampling frequency (Hz) | 100k |
| Analysis frequency range (Hz) | 2500 |
| Fitting model | Polynomial Model |
| Model order | 9 |

Table 6.14 Location of the amplitude peak of 30 repeated tests results for ER 80-04

| Flow rate (lpm) | 1st Test (Hz) | 2nd Test (Hz) | 3rd Test (Hz) | 4th Test (Hz) | 5th Test (Hz) |
|---|---|---|---|---|---|
| 1 | 120 | 123 | 118 | 119 | 120 |
| 1.1 | 146 | 147 | 148 | 148 | 146 |
| 1.2 | 169 | 170 | 168 | 169 | 170 |
| 1.3 | 200 | 204 | 199 | 196 | 201 |
| 1.4 | 235 | 243 | 236 | 237 | 236 |
| 1.5 | 276 | 275 | 277 | 281 | 275 |
| 1.6 | 307 | 309 | 301 | 307 | 301 |
| 1.7 | 332 | 331 | 340 | 340 | 340 |
| 1.8 | 361 | 360 | 355 | 355 | 360 |
| 1.9 | 414 | 405 | 428 | 418 | 401 |
| 2 | 435 | 425 | 429 | 444 | 430 |
| 2.1 | 446 | 452 | 463 | 470 | 456 |

Table 6.15 Analysis of the average peak frequency and the concentration of the data

| Flow rate (lpm) | 1 | 1.1 | 1.2 | 1.3 | 1.4 | 1.5 | 1.6 | 1.7 | 1.8 | 1.9 | 2 |
|---|---|---|---|---|---|---|---|---|---|---|---|
| Average (lpm) | 120 | 147 | 169.2 | 200 | 237.4 | 276.8 | 305 | 336.6 | 358.2 | 413.2 | 432.6 |
| STD | 1.673 | 0.894 | 0.748 | 2.607 | 2.870 | 2.227 | 3.346 | 4.176 | 2.638 | 9.579 | 6.529 |

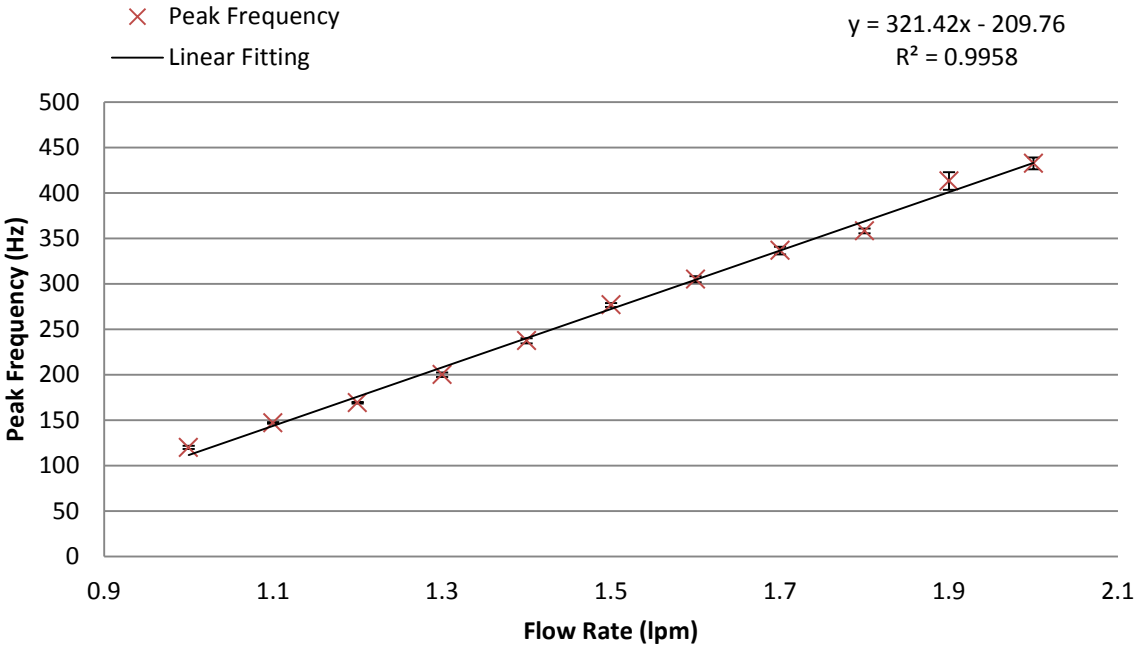


Fig 6.9 Model of the trend of the peak frequency of ER 80-04(with error bars)

## 6.4 SR 80 Series results

### 6.4.1 SR 80-04

The SR 80-04 was the smallest nozzle tested in SR 80 series. The tested flow rate was from 1.0 lpm to 2.1 lpm with 0.1 lpm interval.

Table 6.16 shows the test and data processing condition. Table 6.17 shows the results for 5 repeated tests.

Table 6.16 Test and analysis condition for SR 80-04

| | |
|---|---|
| Microphone | CUI CMP-5247TF-K |
| Distance (cm) | 1.5 |
| Sampling frequency (Hz) | 100k |
| Analysis frequency range (Hz) | 2500 |
| Fitting model | Polynomial Model |
| Model order | 9 |

Table 6.17 Location of the amplitude peak of five repeated tests results for SR 80-04

| Flow rate (lpm) | 1st Test (Hz) | 2nd Test (Hz) | 3rd Test (Hz) | 4th Test (Hz) | 5th Test (Hz) |
|---|---|---|---|---|---|
| 1 | 137 | 137 | 135 | 138 | 137 |
| 1.1 | 151 | 146 | 148 | 147 | 148 |
| 1.2 | 164 | 164 | 165 | 165 | 168 |
| 1.3 | 185 | 187 | 184 | 185 | 185 |
| 1.4 | 214 | 213 | 202 | 210 | 208 |
| 1.5 | 238 | 238 | 233 | 241 | 240 |
| 1.6 | 275 | 285 | 275 | 267 | 280 |
| 1.7 | 315 | 306 | 312 | 313 | 315 |
| 1.8 | 349 | 350 | 352 | 343 | 350 |
| 1.9 | 392 | 382 | 395 | 392 | 391 |
| 2 | 435 | 430 | 428 | 427 | 424 |
| 2.1 | 489 | 480 | 485 | 474 | 476 |

Table 6.18 Analysis of the average peak frequency and the concentration of the data

| Flow rate (lpm) | 1 | 1.1 | 1.2 | 1.3 | 1.4 | 1.5 | 1.6 | 1.7 | 1.8 | 1.9 | 2 | 2.1 |
|---|---|---|---|---|---|---|---|---|---|---|---|---|
| Average (lpm) | 133.4 | 147.6 | 165.6 | 188.4 | 215 | 245 | 280.6 | 317.2 | 350.8 | 392.4 | 430 | 480.8 |
| STD | 6.770 | 1.854 | 2.244 | 6.374 | 11.31 | 15.218 | 11.689 | 11.788 | 5.4918 | 6.1514 | 2.756 | 5.564 |

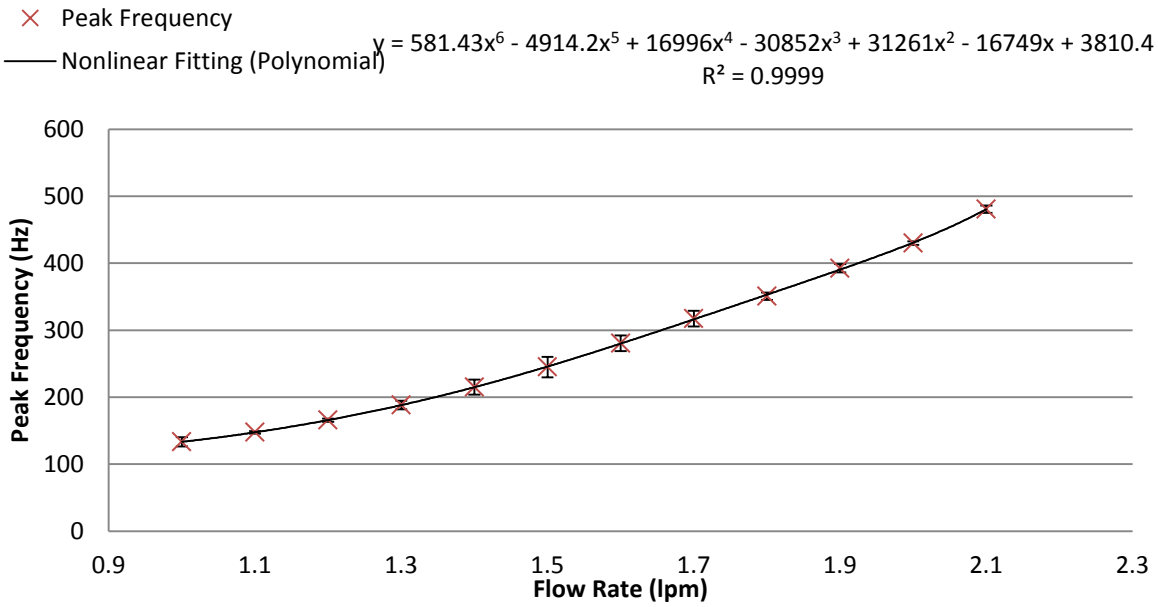


Fig 6.10 Model of the trend of the peak frequency of SR 80-04(with error bars)

## 6.5 Summary and Conclusions

The above experiments include the use of four sizes of MR series nozzle tips, one each of an SR, MR, and ER nozzle tip in a single size. All of the tests were done with the same microphone at a constant distance from the nozzle tip, which was 1.5 cm. With five repeated tests of each nozzle tip, it demonstrated a definite correlation of the frequency with the applicable flow rates individually.

All the curves are shown in the below graph (Fig 6.11)

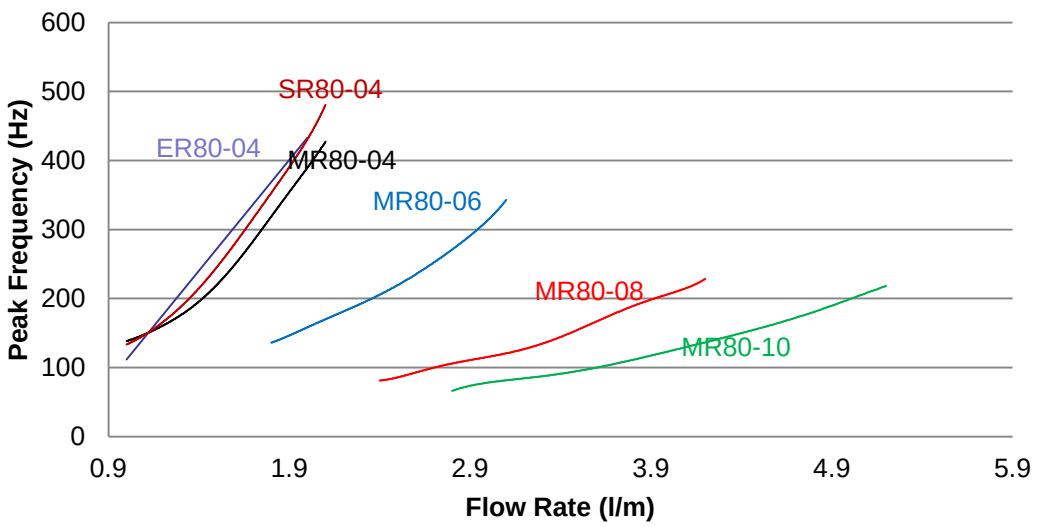


Fig 6.11 Summary of the fitting curves for all the test nozzle tips

The polynomial fitting method was used to fit the frequency response curve. For the MR series nozzle tips, the $6^{th}$ order polynomial equations returned the largest R Square value. The coefficients of the polynomials were different for the different nozzles. The linear fit function was given for the ER 80-04 nozzle for the maximize R square. For the SR 80-04 nozzle tip, a nonlinear polynomial equation with $6^{th}$ order has also been given.

Thus from the results, the techniques used in previous chapters worked for the other nozzle tips, which means there is a definite correlation of the frequency response to the flow rate at a certain distance. For different tip types, there would be different fitting equations.

# Reference


- ADIS16228: DIGITAL TRIAXIAL VIBRATION SENSOR WITH FFT ANALYSIS AND STORAGE. Available at: http://www.analog.com/en/mems-sensors/mems-accelerometers/adis16228/products/product.html.. Accessed 7th, Dec, 2014.
- Alabama A&M and Auburn Universities, and Tuskegee University, County Governing Bodies and USDA Cooperating, August, 2011. Automatic Section Control (ASC) Technology for Agricultural Sprayers.
- Asyiddin,N. 2007. Fluid Flow Measurement, 7. Available at: http://piyushpanchal2007.mynetworksolutions.com/images/3._FLOW.pdf. Accessed 5th, Nov, 2014.
- Balaje Dhanram Ravichandran, 2012. Development of Acoustic Sensor for Flow rate monitoring. MS thesis. Phoenix, AZ: Arizona State University, Department of Electronic Engineering.
- Evans, R.P., J. D. Blotter, A.G. Stephens, 2004. Flow Rate Measurements Using Flow-Induced Pipe Vibration. Journal of Fluids Engineering, Transactions of the ASME, pp280-285.
- Frenzel,F. Grothey,H. Habersetzer,C. Hiatt,M. Hogrefe,W. Kirchner, M. Lütkepohl,G. Marchewka, W. Mecke, U. Ohm, M. Otto, F. Rackebrandt, K. Sievert, D. Thöne,A. Wegener,H. Buhl, F.Koch, C. Deppe,L. Horlebein, A. Schüssler, L. Pohl,U. Jung,B. Lawrence,H. Lohrengel,F. Rasche,G. Pagano,S. Kaiser, A. Mutongo, T. 2011. Industrial Flow Measurement Basics and Practice. ABB Automation Products.
- Fischer,A.Wilke,U. Schlüßler,R. Haufe,D.Sandner,T. Czarske,J. 2014. 17th International Symposium on Applications of Laser Techniques to Fluid Mechanics. Lisbon, Portugal.
- John, 2013. Flow Measurement. Available at: http://www.instrumentationtoday.com/flow/. Ultrasonic Flowmeter. Accessed 5th , Nov, 2014.

- Kakuta,H. Watanabe,K. and Kurihara,Y. 2012. Development of Vibration Sensor with Wide Frequency Range Based on Condenser Microphone-Estimation System for Flow Rate in Water Pipes. World Academy of Science, Engineering and Technology.
- Kumar, S. 2008. Introduction to Measuring Techniques for Fluid Flow Investigations. Indo-German Winter Academy 2008.
- Mattar,W and James Vignos,J. Vortex Shedding Tutorial. Foxboro, Invensys.
- Nick, 2012. Flow Measurement. Available at: http://www.instrumentationtoday.com/flow-measurement/2012/09/. IT Instrumentation-Electronics. Accessed 5th , Nov, 2014.
- Kim, Y. Kimb,Y. 2002. A measurement method of the flow rate in a pipe using a microphone array. J. Acoust. Soc. Am., Vol. 112, No. 3, Pt. 1, Acoustical Society of America.
- KaileidaGraph. *Curve Fitting Guide: The KaileidaGraph Guide to Curve Fitting*. Ver 4.5. Synergy,INC.
- Universal Flow Monitors. Propeller Flowmeter Technology. http://www.flowmeters.com/propeller-technology. Accessed 5th, Nov, 2014.
- Wikipedia Web Site. Available at: http://en.wikipedia.org/wiki/Curve_fitting。 Accessed 5th, Nov, 2014.
- Yoder, 2010. Understanding Vortex Flow Measurement.

# Vita
# Yue Zhang

## Education

2012.08-Master Degree of Biosystem and Agricultural Engineering. University of Kentucky.
2008.09-2012.06. Bachelor Degree of Mechanical Engineering. University of Electronic Science and Technology of China (UESTC).

## Related Experience

**CNH Grant:** Control and Monitoring of Sprayer Output ***2013.08 -2014.08***

**NSF Grant:** Nonlinear Modeling and Tracking Control of 3D Weld Pool in GTAC ***2013.12-2014.01***

**Research Topic:** Seeking solution for the Two-Node Decentralized LQR Problem ***2012.10-2013.05***

**National College Innovation Fund:** Serpentine Robot ***2010.10-2011.10***

**National-Semiconductor Project:** Auto Handling Robotcar ***2010.06-2010.12***

## Career History

**Research Assistant,** *BAE Department, University of Kentucky* ***2013.08 -2014.08***

**Part-time Research Assistant,** *Welding Research Lab, University of Kentucky* ***2013.12 -2014.01***

**Teaching Assistant,** *ME Department, University of Kentucky* ***2012.08 -2013.06***

**Intern,** *Marvell Semiconductor, Shanghai, China* ***2011.06-2011.09***

**Research Assistant,** *Sino-Japan Remote Joint Robotics Lab, Chengdu, China*

***2010.09- 2011.10***